PERTURBATIVE IMPROVEMENT OF LATTICE GAUGE ACTION WITH STAGGERED QUARKS

by

Zhihao Hao

B.Sc., Tsinghua University, 2004

THESIS SUBMITTED IN PARTIAL FULFILLMENT

OF THE REQUIREMENTS FOR THE DEGREE OF

MASTER OF SCIENCE

IN THE DEPARTMENT

OF

PHYSICS

SIMON FRASER UNIVERSITY

Fall 2006

APPROVAL

Name: Zhihao Hao

Degree: Master of Science

Title of Thesis: Perturbative Improvement of Lattice Gauge Action with Staggered Quarks

Examining Committee: Prof. Karen L. Kavanagh (Chair)

Dr. Howard D. Trottier
Senior Supervisor
Professor, Department of Physics

Dr. Richard M. Woloshyn
Research Scientist
TRIUMF

Dr. Byron Jennings
Research Scientist
TRIUMF

Dr. Malcolm Kennett
Internal Examiner
Assistant Professor, Department of Physics

Date Approved: August 23rd, 2006

Abstract

Realistic unquenched Lattice QCD including dynamical fermions has become available thanks to the use of highly improved staggered quarks and other newly developed techniques. While these calculations yielded excellent agreement with experiments, unquenched studies of the static quark potential at short distances show larger discretization errors than in quenched simulations. At leading order in perturbation theory these errors arise from $O(\alpha_s a^2)$ corrections to the couplings in the lattice gauge action (α_s is the QCD coupling and a is the lattice spacing); fermion loop contributions to these couplings have not previously been available.

In this thesis, fermion loop contributions to $O(\alpha_s a^2)$ improvement of the gauge action are calculated. The approach developed by Lüscher and Weisz is adopted and reviewed in detail. It is observed that dynamical contributions are large and hence can be the source of the large scaling violations in previous simulations of the unquenched static potential.

To my parents

Acknowledgments

I owe the two wonderful years in SFU and TRIUMF to many people. First and Foremost I want to thank Howard D. Trottier for teaching me so much about Quantum Field theory, lattice QCD and Particle Physics in general, for his appreciated help without which the current work is impossible and above all for his trust and constant encouragement during all this time. Many thanks to Richard M. Woloshyn for discussions from which I learned a lot. I also want to thank John N. Ng for teaching me so many things about particle physics and for inspirations on research methods and projects. Dr. Leslie Ballentine is thanked for his instructions in my course work in SFU. I also owe the initial discovery of my research interest to Leslie.

A lot of help come from colleagues from SFU, TRIUMF and HPQCD collaboration. I benefited a lot from the notes of Ronald R. Horgan and Georg M. von Hippel. I want to thank Jackson Wu for many helpful discussions. Yi Deng, Yang Guo and Michael Steger are specially thanked for their friendships which form an important part of my life in Vancouver. I also want to take the opportunity to thank my parents for their love and support.

Finally, thanks to all the people I have been working with and interacting with these two years, it's all of you who make the past two years so memorable.

Contents

List of Tables

List of Figures

Chapter 1

Introduction

The standard model of particle physics is one of the most successful physical theories. It has stood up against thirty years' experimental tests ever since its birth[1]. However, not only have hints for physics beyond standard model[2] been accumulating, there are also vast territories within the standard model remaining to be explored. The chapter is dedicated to present an updated general picture of particle physics and a general description of the Standard Model. A brief introduction to non-perturbative aspects of strong interactions and Lattice QCD is also included. Finally, chiral symmetry and its breaking are described and their importance to low energy physics and lattice QCD is indicated.

1.1 Current picture of Particle Physics and the Standard Model

The fundamental building blocks of our universe can be categorized into two species, namely fermions and bosons. Fermions obey Fermi-Dirac statistics and have half-integer spins. In contrast bosons are governed by Bose-Einstein statistics and possess integer spins. According to the Standard Model(SM), there are 3 generations of fermions and 12 gauge bosons at the fundamental level[1].

[1]Nowadays particle physics community generally regards SM as a effective field theory at low energy. However, since no new degree of freedom has been established through clear-cut experimental evidence, I will stick to a more conservative point of view.

Table 1.1: Numbers in $SU(3)_c$ and $SU(2)_L$ sections denote transformation properties of corresponding particles under certain group. For example, u_R transform as both a $SU(3)_c$ *triplet* and a $SU(2)_L$ *singlet*. Numbers in $U(1)_Y$ give the corresponding hypercharges.

Particle	$SU(3)_c$	$SU(2)_L$	$U(1)_Y$
$\begin{pmatrix} u \\ d \end{pmatrix}_L$	3	2	$\frac{1}{6}$
u_R	3	1	$\frac{2}{3}$
d_R	3	1	$-\frac{1}{3}$
$\begin{pmatrix} \nu \\ e \end{pmatrix}_L$	1	2	$-\frac{1}{2}$
e_R	1	1	-1
ϕ_{Higgs}	1	2	$\frac{1}{2}$

Each generation of fermions contains 2 quarks, a charged lepton and a neutrino. In the SM, particles of different chirality are regarded as different particles. Taking into account of the fact that there are no right handed neutrinos in the SM, there are 7 chiral fermions within a generation. Corresponding fermions in different generations possess identical quantum numbers except for mass. The generation structure can't be explained within the standard model and remains one of the most fascinating questions in particle physics. The first generation of fermionic degrees of freedom in the SM are summarized in table 1.1.

There are two kinds of interactions between fermions. The strong interaction exists between quarks and is mediated by 8 kinds of gluons of different colors. The electro-weak(EW) interaction occurs universally between fermions. Above the EW symmetry breaking scale, the interaction is mediated by 4 massless bosons. Below the scale, the symmetry is broken to $U(1)$ symmetry for Quantum Electrodynamics(QED). While the photon remain massless, the other three bosons become massive W^+, W^- and Z bosons.

The form of the SM Lagrangian is tightly constrained by Lorentz invariance and gauge symmetry $SU(3)_c \otimes SU(2)_L \otimes U(1)$. The $SU(2)_L \otimes U(1)$ gauge group is responsible for

the EW interaction. The gauge symmetry is broken minimally by a Higgs doublet, which forms a fundamental representation of $SU(2)_L$. Within each generation, left-handed quarks and left-handed leptons form fundamental representations of $SU(2)_L$ respectively while the right-handed counterparts are $SU(2)_L$ singlets. Each one of doublets and singlets has a particular $U(1)$ charge. The EW sector of the standard model has passed extensive experimental tests at B factories, LEP, HERA and Tevatron with percentage accuracy[1]. The Higgs sector remains to be discovered and studied. The relevant energy regions are to be explored in LHC[3].

The $SU(3)_c$ generates Quantum Chromo-dynamics(QCD), the theory for strong interactions. QCD reconciles the infrared confinement and the ultraviolet asymptotic freedom into a simple and consistent theory. The gauge coupling of strong interactions g_s runs with the characteristic energy scale of the physical system of interest. The energy range in which $\alpha_s \equiv g_s^2/(4\pi) < 1$ is called the perturbative region of QCD while in the non-perturbative region of QCD, $\alpha_s \geq 1$. The energy scale separating the perturbative and the non-perturbative regions of QCD is usually denoted as Λ_{QCD}. Concrete experimental evidence for QCD comes mostly from perturbative region of QCD. The non-perturbative aspect of QCD will be described in next section.

There are also some discrete symmetries and "accidental" symmetries[4] present in the SM. Parity(P) reverses the spatial coordinates, time reversal(T) flips the time coordinate while charge conjugation(C) changes particle to antiparticle. The QCD Lagrangian is invariant under C, P, T respectively while the EW Lagrangian respects only CP and T. The combination operation of CPT is believed to be a fundamental symmetry of the SM. Given the degrees of freedom in the SM, baryon number and 3 kinds of lepton numbers(electron, muon, τ) are conserved accidentally. In fact, some models beyond the SM predicts baryon number and lepton number violating processes.

All in all, the SM is deduced from a limited number of basic principles and explains natural phenomena in a vast range of energy scales. It is certainly a remarkable triumph of human intellectual exploration. However, some big questions are still left unanswered like the famous fermion mass problem and the hierarchy problem[5]. Hopefully new discoveries and breakthroughs would be achieved through the next generation experiments.

1.2 Non-perturbative aspect of QCD and Lattice QCD

Ironically, as the theory of strong interactions, QCD was established and tested mostly by experiments performed in the perturbative region where the strong interactions are "weak"($\alpha_s < 1$). It doesn't mean that the non-perturbative aspects of strong interactions are of little interest to us. Actually, the situation is quite the opposite. There are many both fascinating and important questions to be answered in this field.

First of all, the non-perturbative aspects of strong interactions is of great theoretical interest. As α_s becomes larger than 1, two interesting phenomena take place. One of them is the famous color confinement[6]. Below Λ_{QCD} there are no free quark or gluon degrees of freedom. All the colors are confined into colorless hadrons and mesons. While indications of confinement were obtained by Lattice calculation[6], a clear understanding of its mechanism is still absent. The other interesting phenomena is chiral symmetry breaking[7]. The breaking of chiral symmetry is essential for the establishment of low energy effective theories such as chiral perturbation theory. It is also a good chance for us to understand the dynamics of symmetry breaking in particle physics. In order to appreciate the problem and also for later reference, a brief introduction to chiral symmetry and its breaking in QCD will be presented in Section 1.4. Of course, there are other very interesting questions such as the topology of QCD vacuum, the QCD superconductivity and the quark gluon plasma[8].

Secondly, an effective way to handle non-perturbative QCD is very important if we want to address a lot of relevant experimental and phenomenological problems. The ongoing quest of measurements of CKM matrix elements[9] rely heavily on semi-leptonic and leptonic decays of meson, where various form factors are essentially non-perturbative QCD quantities. There are also some "exotic" particles predicted by QCD like glueballs[10] and hybrid mesons whose existence and properties can be determined by clear well-understood non-perturbative calculations.

First proposed by Wilson[11], lattice QCD(LQCD) is one of the most well-established and effective tools to explore the non-perturbative aspect of QCD. By replacing continuous Minkowski space-time with a finite Euclidean hyper-cubic lattice, the number of degrees of freedom is reduced to be finite so that statistical Monte-Carlo methods are applicable. Gauge symmetry is preserved rigorously while Lorentz symmetry is broken down to 4 dimensional hyper-cubic symmetry. Ideally, a calculation is performed on lattices of different

lattice spacing a and an extrapolation to zero lattice spacing will be performed in order to get the continuum limit, which implies that the finer lattice spacing is preferred. However, our ability to reduce lattice spacing given a specific problem is severely constrained by available computer power. Therefore in order to get results with a certain accuracy on relatively coarse lattice, various improvement schemes of the discretized QCD lagrangian are adopted by the lattice community. A good deal of effort has been focused on improving the convergence of lattice calculation results as a decreases by perturbatively removing the higher order lattice artifacts in lattice QCD Lagrangians.

1.3 A sketch of the goal

As was pointed out in the previous section, perturbatively improved lattice actions have become indispensable for high precision lattice QCD calculations. Lattice QCD is an effective theory which excludes high-energy modes beyond the lattice cutoff $\sim \pi/a$, and whose contributions to physical amplitudes in the continuum theory are therefore missing in a naive lattice discretization. One can use perturbation theory to compensate for the effects of these high-energy modes by including irrelevant operators in an "improved" lattice discretization; the strength of these operators can be computed by matching a set of scattering amplitudes in the lattice theory to the corresponding results in the continuum, order by order in an expansion in $\alpha_s(q^*)$, at a scale $q^* \sim \pi/a$. Generally speaking the discretization errors in a lattice calculation can be expanded in terms of $a\Lambda_{QCD}$ and α_s. Λ_{QCD} is roughly $250MeV$ and a is typically $0.1fm$. Therefore $a\Lambda_{QCD}$ is around $0.2-0.3$. α_s at the scale of reverse lattice spacing here is also of the same range. In order to achieve few percent accuracy, we need only perform our perturbative improvement of the lattice action to order $(a\Lambda_{QCD})^2$, α_s^2 and $\alpha_s a\Lambda_{QCD}$. It's in fact usually the goal of the HPQCD(High precision QCD) collaboration.

Following the same argument, order $\alpha_s a^2$ improvement considered by Lücsher and Weisz[12] is generally not needed for the HPQCD collaboration . However, Christine T. H. Davies and her team[13] have analyzed simulations of the heavy quark potential using the Lüscher-Weisz gauge action with the presence of dynamical quarks. They found that the scaling violations is somewhat larger than the scaling violations in the quenched case, which is contradictory to the conventional wisdom that by introducing quark loop effects

the simulation result should be more continuum like. A first possible answer to the problem is that the missing sea quark contributions to the improvement coefficients in the Lüscher-Weisz action will reduce the scaling violations to be at least comparable to the quenched case. Our work here is trying to find out whether the possible error source can explain the large scaling violations observed.

As will be clear latter, the "complete" improvement coefficients are the sums of gluon contributions, ghost contributions and quark contributions. Since the non-quark contributions are well-established by the calculations of Lüscher and Weisz[12], we only calculate the quark loop contributions here. We pursue only the on-shell improvement[14] which is designed to cancel out the scaling violations only in on-shell quantities and was also invented by Lüscher and Weisz. The detail of the approach will be reviewed in Chapter 4. It was shown that if one pursues only order $\alpha_s^n a^2 (n = 0, 1 \ldots)$ improvement there are mere two dimension six operators with independent coefficients needed in the counter-term. We then perform the improvement by calculating the one-loop contributions to two independent on-shell quantities and tuning the coefficients of the counter-terms to cancel out the order a^2 scaling violations within.

It was also pointed out by Lüscher and Weisz that one loop calculations of on-shell quantities in four dimensional Euclidean space-time are too complicated to implement in lattice perturbation theory. They proposed to carry out the calculation in the "twisted world" in which two directions of space-time are compactified and twisted periodic boundary conditions[2] are imposed. The special geometrical setting generates a tower of "mesons" which are just gluons of different minimum momentum modes. Among these mesons, the two with lowest and the second lowest minimum momentum modes, namely A and B meson, remain stable when interactions are turned on. A set of new on-shell quantities are therefore available and we choose the minimum momentum mode of A meson as well as the phenomenological coupling between two A mesons and one B meson as our two on-shell quantities.

Readers shouldn't be bothered to feel confused after the present section. There is a lot of information presented with details due in following chapters. One needs only keep in mind the big picture. The second chapter will give a detailed review of Lattice QCD formalism in general. Lattice perturbation theory and twisted periodic boundary conditions will be

[2]Twisted periodic boundary conditions will be reviewed in detail in Section 3.3.

reviewed in Chapter 3. We will introduce the idea of on-shell improvement in Chapter 4. The quenched calculation done by Lüscher and Weisz as well as Snippe will be reviewed in the same chapter. In Chapter 5 the current calculation of previously uncharted quark loop contributions is described and results are summarized. Finally in the last chapter the results are discussed and the conclusion is drawn.

1.4 Chiral symmetry and its breaking in QCD

Before moving on to Chapter 2, a brief account for chiral symmetry and its breaking in QCD is necessary for future reference and also for its own importance. First, let's take a look at the QCD Lagrangian:

$$L_{QCD} = -\frac{1}{4}F_{\mu\nu}F^{\mu\nu} + \sum_q \overline{q}\left(iD_\mu\gamma^\mu + m\right)q, \tag{1.1}$$

where $D_\mu = \partial_\mu - igA^a_\mu T^a$, $F_{\mu\nu} = \partial_\mu A_\nu - \partial_\nu A_\mu + ig[A_\mu, A_\nu]$ and q denotes different quark flavors. T^a's are $SU(3)$ generators. Γ_μ is the Dirac matrix and A_μ is the vector gauge field.

If we concentrate on the quark sector of the Lagrangian and consider the massless limit, the Lagrangian can be decoupled into a left part and a right part[3]:

$$L = \sum_q i(\overline{q_L}D_\mu\gamma^\mu q_L + \overline{q_R}D_\mu\gamma^\mu q_R), \tag{1.2}$$

where $q_L = \left(\frac{1-\gamma^5}{2}\right)q$ and $q_R = \left(\frac{1+\gamma^5}{2}\right)q$. It is clear that the Lagrangian is invariant under rotations independently applied on left field and right field. In the other word, classical massless QCD is invariant under $U(3)_L \otimes U(3)_R$. Symmetries can be rewritten as $U(1)_V \otimes U(1)_A \otimes SU(3)_L \otimes SU(3)_R$. $U(1)_V$ is responsible for conservation of baryon number while $U(1)_A$ is broken due to anomalies as the theory is quantized. In the perturbative region, the $SU(3)_L \otimes SU(3)_R$ symmetry is present. However, it is inferred from experimental facts that the symmetry is broken down to $SU(3)_V$ in the non-perturbative region. The mechanism of the symmetry breaking is still unknown.

Chiral symmetry and its breaking have very profound physical implications. First of all, a BCS-like understanding of the dynamics of symmetry breaking will bring our understanding of symmetry breaking in particle physics to a complete new level. Secondly,

[3]Regarding to properties of gamma matrices one can refer to [16]

$SU(3)_V$ present in the low energy physics imposes strong constraints on the forms of effective field theories in low energy region. The celebrated success of chiral perturbation theory is a good example. A lattice fermion Lagrangian should also respect chiral symmetry to a certain extent if the Lagrangian is going to impact phenomenology.

Chapter 2

A brief review of Lattice QCD

Pioneered by Wilson[11], Lattice QCD(LQCD) is almost as old as QCD. After decades of development[15], LQCD is one of the most effective tool to explore non-perturbative aspects of QCD. There are various applications ranging from highly theoretical interest like non-perturbative definition of chiral symmetry to phenomenological interests. The present chapter is intended to give a brief description of lattice formalism as well as a simple account of its problems and applications.

2.1 A General introduction

LQCD is based on several general ideas. First of all, functional quantization of QCD allows the possibility to solve QCD numerically. According to the path integral formalism[16], the expectation value of an operator O can be calculated as following:

$$< O >= \frac{\int DAD\psi D\bar{\psi} O e^{i\int d^4xL}}{\int DAD\psi D\bar{\psi} e^{i\int d^4xL}}, \tag{2.1}$$

where L is the QCD Lagrangian1.1. A particular field, say gauge field A, at a specific space-time point is an *independent* integration variable. Effectively in 2.1 we average operator O over all possible field configurations weighed by corresponding exponential factors. For continuum space-time, there are an infinite number of degrees of freedoms to integrate over and a numerical treatment is impossible. However, if continuum space-time is replaced with a discrete lattice and a finite volume is adopted, the number of degrees of freedoms becomes

finite and a numerical treatment is feasible in principle. This is the most naive picture of LQCD. However, it's also transparent that when the action $S = \int d^4xL$ is large the exponential factor will oscillate rapidly. If a lattice calculation is carried out in the naive way as suggested, there would be a lot of cancelations between different contributions, which would be a great waste of computer power. Furthermore there is a more serious problem: generic poles exist in Minkowski correlation functions so that the naive integration would just blow up.

The above difficulties necessitate the second ingredient: Euclidean space-time field theory[17]. A quantum field theory formulated in Minkowski space-time can be analytically continued to Euclidean space-time by Wick Rotation:

$$x_0 \rightarrow -ix_4. \tag{2.2}$$

Let's consider Klein-Gordon scalar QFT as an example. The Minkowski space-time Lagrangian reads:

$$L = \frac{1}{2}\partial_0\phi\partial_0\phi - \sum_{i=1}^{3}\frac{1}{2}\partial_i\phi\partial_i\phi - m^2\phi^2. \tag{2.3}$$

The theory can be quantized using a functional method similar to 2.1. After Wick Rotation, the functional formula undergoes following the changes:

$$\begin{aligned} &i\int dtd^3x \rightarrow \int d^3xdx_4, \\ &L_M \rightarrow -(\frac{1}{2}\partial_4\phi\partial_4\phi + \sum_i \frac{1}{2}\partial_i\phi\partial_i\phi + m^2\phi^2) = -L_E. \end{aligned} \tag{2.4}$$

These generic relations are also true for QCD. The expectation value of an operator O now reads:

$$< O >= \frac{\int DAD\psi D\bar{\psi}O_E e^{-\int d^4x_E L_E}}{\int DAD\psi D\bar{\psi}e^{-\int d^4x_E L_E}}, \tag{2.5}$$

where the subscript E is used to distinguish Euclidean operators from Minkowski operators. Equation 2.5 bears close similarity to a calculation of the expectation value of a correlation function in statistical mechanics. This observation enables us to apply well-developed Monte-Carlo methods. The legitimacy of the analytical continuation was shown in the context of perturbation theory by Wick and Schwinger[18]. However, its applicability in the non-perturbative region is an unproven *assumption*. Euclidean field theory can

also be constructed independent of a counterpart in Minkowski space and it is interesting by itself. However, for our purposes it is only necessary to notice that the Lagrangian of Euclidean field theory is positive definite and divergence free.

A bit more discussion about the Wick rotation is necessary for future reference. The common statement that Wick rotation transforms a quantum field theory in Minkowski space into a quantum field theory in Euclidean space is misleading. In fact, forced by the pole structure in complex p_0 plane, 2.2 implies p_0 should be rotated to the opposite direction. One can convince oneself that it's the case by observing the fact that operator corresponding to p_0 is proportional to ∂_0 which rotates the opposite way to x_0. It is natural that A_0 transforms the same way as ∂_0 given their same footing in the definition of covariant derivative. Summing these up, we have

$$\begin{aligned} x_0 &\rightarrow -ix_4 \\ p_0 &\rightarrow ip_4 \\ A_0 &\rightarrow iA_4. \end{aligned} \tag{2.6}$$

Notice that $k_0x_0 - \vec{k}\cdot\vec{x}$ transforms to $k_4x_4 - \vec{k}\cdot\vec{x}$ which is not a Euclidean $O(4)$ invariant. However, for a pure gauge field, the argument of the plane wave function $e^{ik\cdot x}$ can be replaced by $ik_E \cdot x_E = \sum_{i=1}^{4} k_i x_i$.

Thirdly, it is important to notice that the lattice is a way to regularize a general QFT non-perturbatively[19]. Generally a QFT is well defined only after a proper regularization scheme is specified. In the perturbative region, regularization is applied perturbatively as a way to cut off the infinities present in loop diagram calculation. A new scale is introduced into the theory once the theory is regularized. An explicit example is Λ_{QCD} in QCD which is introduced into the theory through the $\overline{MS}$ regularization scheme. Lattice regularization introduces a new scale as well, namely the lattice spacing a and the would-be infinities in loop integration are cut off to finite values thanks to the finite size of the Brillouin zone. If not specified, a will be set to 1 and it will be assumed that every dimensionful quantity is scaled by proper powers of a and becomes dimensionless in the following sections. It is equally important to notice that lattice regularization is applied at the level of Lagrangian and is therefore independent of perturbation theory. Lattice regularization is the only known non-perturbative regularization which is gauge invariant.

In addition, symmetries are as important as in other physical systems. By introducing

a 4-dimensional hyper-cubic lattice, space-time Lorentz symmetry(Poincaré group) is reduced to the discrete hyper-cubic group. However, as the continuum limit is taken Lorentz symmetry will be recovered. Local gauge invariance is preserved on the lattice by using a link field as gauge degrees of freedom as will be discussed in detail in Section 2.3.1.

Finally, a lattice action should yield the right continuum theory, say QCD, as $a \to 0$. For finite lattice spacing, the difference between lattice quantities and their true physical values will be of the order of powers of ap where p is the typical scale of physical process we are considering. Normally p is much less than $\frac{\pi}{a}$. Ideally errors relative to continuum theory induced by lattice spacing can be extrapolated away by reducing a. However, the computer power available now is not enough for such a straightforward approach. As a result, various improvement programmes are invoked to reduce the effects of lattice artifacts.

The following sections of this chapter will show step by step how lattice regularization is applied and how gauge invariance is preserved. In Section 2.5 a combined picture of lattice QCD will be given. An introduction to lattice perturbation theory will be presented in the Section 2.6 and various sources of errors will be reviewed in the last section.

2.2 Local Gauge invariance

Before we move on to explicit construction of lattice QFT, it is instructive to review the implementation of local gauge invariance in continuum QFT's[1]. It will serve as the reference and basis for the realization of gauge invariance on the lattice. Building blocks of LQCD will also be introduced.

Local gauge invariance is one of the key ideas behind the Standard Model. It is deeply connected to locality and unitarity of a quantum field theory, both of which have in turn been corner stones of physics since the revolution of Quantum Mechanics and Special Relativity. There is also an intrinsic relation[20] between local gauge invariance and the celebrated CPT theorem. All of these add up to the essential importance of gauge symmetry.

In the Abelian case, the principle can be stated as follows: the Lagrangian of a proper theory should be invariant under transformation $\psi \to e^{i\alpha(x)}\psi$ where ψ is a generic fermion field. It is apparent that $m\bar{\psi}\psi$ is gauge invariant. In order to construct gauge invariant

[1] A more detailed account of local gauge symmetry can be found in Chapter 15 of [16]

operators involving derivatives, a comparator field $U(x,y)$ is introduced[2] which transforms as follows:

$$U(x,y) \to e^{i\alpha(x)}U(x,y)e^{-i\alpha(y)}. \tag{2.7}$$

Now we can define covariant derivative of ψ:

$$D^{\mu}\psi(x) = \lim_{a\to 0}\frac{1}{a}(\psi(x+a) - U(x+a,x)\psi). \tag{2.8}$$

It can be shown that $D^{\mu}\psi(x)$ transforms the same way as $\psi(x)$. The comparator field can be parameterized as

$$U(y,x) = P(e^{-ie\int_x^y dx_{\mu}A^{\mu}(x)}), \tag{2.9}$$

where $A(x)$ is identified as the gauge field and P stands for path ordering operator. As one can see in detail in [16], by defining $U(y,x)$ as in 2.9 and requiring it to transform as a gauge group element as in 2.7 $A_{\mu}(x)$ transforms like $A_{\mu}(x) \to A_{\mu}(x) - 1/e\partial_{\mu}\alpha(x)$, which is the standard Maxwell gauge transformation for EM gauge fields. Given $D_{\mu}\psi$ transforms the same way as ψ, the operator $\bar{\psi}\gamma^{\mu}D_{\mu}\psi$ is gauge invariant as well. Taking the limit as $a \to 0$, $\bar{\psi}\gamma^{\mu}D_{\mu}\psi + m\bar{\psi}\psi$ becomes the familiar QED Lagrangian.

One might notice that $\bar{\psi}(x+a)U(x+a,x)\psi$ is gauge invariant by itself. More generally, a "line" operator is gauge invariant if it's of the following form:

$$\bar{\psi}(x_n)U(x_n,x_{n-1})\cdots U(x_j,x_{j-1})\cdots U(x_2,x_1)\psi(x_1), \tag{2.10}$$

where $j = 2,3\ldots n$.

For a pure gauge action, the continuous gauge invariant form $F_{\mu\nu}$ is related to the "loop" operator in the following way:

$$\begin{aligned} &U(x,x+a\hat{\mu})U(x+a\hat{\mu},x+a\hat{\mu}+a\hat{\nu})U(x+a\hat{\mu}+a\hat{\nu},x+a\hat{\nu})U(x+a\hat{\nu}) \\ &\underset{a\to 0}{=} 1 + iea^2F_{\mu\nu} + o(a^3) + \ldots, \end{aligned} \tag{2.11}$$

where $F_{\mu\nu} \equiv \partial_{\mu}A_{\nu} - \partial_{\nu}A_{\mu}$ and we replaced path ordering integration in 2.9 with $e^{ieA(x+\frac{1}{2}a\hat{\mu})a}$ as $a \to 0$. The gauge invariance of the loop operator is easy to verify. A more general loop can be written in the following form:

$$U(x) = U(x,x_1)U(x_1,x_2)\cdots U(x_j,x_{j+1})\cdots U(x_n,x), \tag{2.12}$$

[2]Be aware that comparator field is now defined in *Minkowski space*. The transition to Euclidean space will be performed latter.

where $j = 1,2\ldots n-1$.

"Loop" and "line" operators introduced above can be easily generalized to the non-Abelian case by replacing $-eA_\mu(x)$ with $gA^a_\mu T^a$ where T^a is the generator of corresponding non-Abelian gauge group. The loop operator $U(x)$ is also redefined as the trace of 2.12:

$$U(x) = Tr(U(x,x_1)U(x_1,x_2)\cdots U(x_j,x_{j+1})\cdots U(x_n,x)). \tag{2.13}$$

All of the above discussion is set in Minkowski space. We can also start from the Euclidean free fermion action and define comparator field in Euclidean space-time. The discussion follows the same line because the gauge group is independent of the space-time symmetry group. We can define the comparator field in Euclidean space as follows:

$$U(y,x) = P(e^{-iag\int_x^y \Sigma_{i=1}^4 dx_i A_i(x)}). \tag{2.14}$$

It transforms similarly to the comparator field in Minkowski space under gauge transformation. It is evident that loops and lines formed by Euclidean comparator fields are gauge invariant as well.

In order to build a continuum gauge invariant theory, we make use of building blocks including the covariant derivative and $F_{\mu\nu}$. Through the above arguments it is noticed that there is a set of equally good gauge invariant building blocks consisting of "line" and "loop" operators. These operators are officially named as the Wilson line and the Wilson loop. They are essential for us to build up a gauge invariant lattice action.

2.3 Bosons on the Lattice

As discussed in Section 2.1 and Section 2.2, a proper lattice action should obey gauge and other lattice symmetries while yielding the correct continuum limit as $a \to 0$. There are nevertheless an infinite number of actions satisfying the two requirements. Unimproved actions usually converge slower to the continuum limit as a approaches zero, resulting in large deviations from the continuum limit while an improved lattice action to certain orders of a generally produces more accurate results with modest computation cost. Therefore construction of a good lattice action is a highly non-trivial issue. Pure gauge actions will be constructed in the present section while fermionic actions will be discussed in the next section with corresponding improvement efforts discussed.

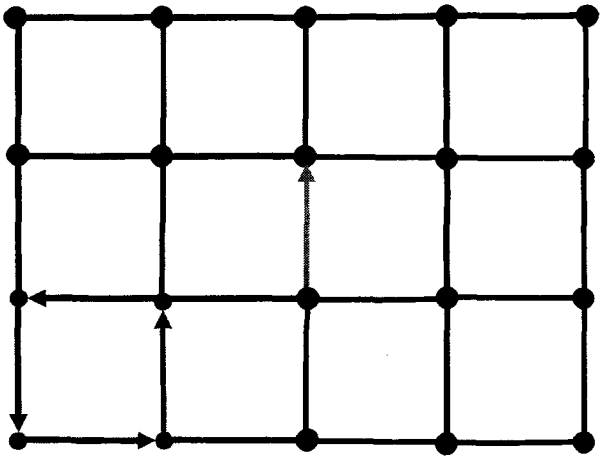

Figure 2.1: The diagram shows a two dimensional lattice. Fermions live on the lattice sites. The single arrow shows an example of link variable U_x. The rectangle consisting of four link fields(arrows) is a plaquette.

2.3.1 The basic formalism

Gauge invariance is the key ingredient in the construction of a lattice version of a pure gauge action. It is essential to preserve Ward identities and universality of the gauge coupling. If we don't preserve gauge symmetry rigorously, every coupling, for example the three gluon coupling and the four gluon coupling, has to be fine tuned independently in the of various operators in order to produce the right continuum limit, which would be an unnecessary complication of the calculation. For this purpose, the continuum gauge-field degrees of freedom are replaced with a "link" field:

$$U_\mu(x) = e^{igA_\mu(x+\frac{1}{2}\hat{\mu})}, \tag{2.15}$$

where we set the lattice spacing to 1 as discussed in Section 2.1. In the non-Abelian case, $A_\mu(x) = A^a_\mu(x)T^a$ where T^a is the generator of the corresponding non-Abelian gauge group. It is apparent that the definition of the link field is closely related to definition of the comparator field in 2.9. If we approximate the path ordering integration in 2.14 to be a product of $A^\mu(x+\frac{a}{2}\hat{\mu})$ and a, after setting $a = 1$ we will get relations between the Euclidean com-

parator field and the link field:

$$\begin{aligned} U(x,x+\hat{\mu})_E &= U_\mu(x)_E, \\ U(x,x-\hat{\mu})_E &= U_\mu^\dagger(x-\hat{\mu})_E. \end{aligned} \tag{2.16}$$

The subscript E will be dropped hereafter. For simplicity of discussion, the Abelian case will be considered in the rest of the section.

Based on the discussion in Section 2.2, we can preserve gauge symmetry rigorously on the lattice if a gauge action consists of the Wilson loops. The simplest Wilson loop on the lattice is a plaquette. A plaquette is defined as the trace of the product of four link fields:

$$P \equiv Re\left(Tr(1-U_\mu(x)U_\nu(x+\hat{\mu})U_\mu^\dagger(x+\hat{\nu})U_\nu^\dagger(x))\right). \tag{2.17}$$

If we make use of relation 2.16, $U_\mu(x)U_\nu(x+\hat{\mu})U_\mu^\dagger(x+\hat{\nu})U_\nu^\dagger(x)$ becomes $U(x,x+\hat{\mu})U(x+\hat{\mu},x+\hat{\mu}+\hat{\nu})U(x+\hat{\mu}+\hat{\nu},x+\hat{\nu})U(x+\hat{\nu},x)$ which is exactly the form of 2.11. The gauge invariance of the plaquette is now evident. Let's restore the lattice spacing a temporarily and expand every gauge field around $x+\frac{a(\mu+\nu)}{2}$. We have:

$$\begin{aligned} W_{1\times1} =& U_\mu(x)U_\nu(x+\hat{\mu})U_\mu^\dagger(x+\hat{\nu})U_\nu^\dagger(x) \\ =& e^{iag(A_\mu(x+\frac{a}{2}\hat{\mu})+A_\nu(x+a\hat{\mu}+\frac{a}{2}\hat{\nu})-A_\mu(x+a\hat{\nu}+\frac{a}{2}\hat{\mu})-A_\nu(x+\frac{a}{2}\hat{\nu}))} \\ =& e^{ia^2g(\partial_\mu A_\nu(x+a(\frac{\hat{\mu}+\hat{\nu}}{2}))-\partial_\nu A_\mu(x+a(\frac{\hat{\mu}+\hat{\nu}}{2}))+O(a^2))} \\ =& 1+i(a^2gF_{\mu\nu}+O(a^4))-\frac{a^4g^2}{2}F_{\mu\nu}F^{\mu\nu}+O(a^6), \end{aligned} \tag{2.18}$$

where we used $W_{1\times1}$ to denote the plaquette. Keep in mind that repeated indices do *not* imply summation here. It is clear that:

$$P_{\mu\nu} = \frac{a^4}{2}g^2Tr(F_{\mu\nu}F^{\mu\nu})+O(a^6). \tag{2.19}$$

Now define the lattice gauge action S_W as:

$$S_W = \beta\sum_{\mu<\nu}\sum_x\frac{1}{3}P_{\mu\nu}, \tag{2.20}$$

where $\beta=\frac{6}{g^2}$ for $SU(3)$ QCD. As $a\to0$, S_W converges to the continuum gauge action with $O(a^2)$ error. The action bears the official name the Wilson gauge action.

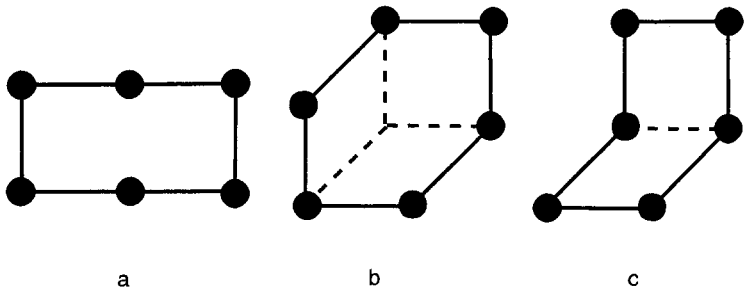

Figure 2.2: A set of three Wilson loops can be added to the gauge action to cancel out $O(a^2)$ scaling violations.

2.3.2 Improvement of the gauge action

It is shown in the previous section 2.3.1 that the Wilson gauge action S_W yields the correct continuum limit up to an $O(a^2)$ correction for the abelian case. As discussed in Section 2.1, it is very desirable to remove at least the leading discretization errors given the insufficiency of today's computer power.

In the non-Abelian case the $O(a^2)$ correction reads[21]:

$$-\frac{a^6}{72}Tr[gF_{\mu\nu}(D_\mu^2+D_\nu^2)gF_{\mu\nu}].$$

This term can be found also in the expansion of a Wilson loop of size 1×2: $R_{\mu\nu}$ whose shape is shown as a in Fig. 2.2. It was also shown by Lüscher and Weisz[14] that in the following definition of gauge action the $O(a^2)$ error can be removed[3]:

$$L=\frac{5}{3}P_{\mu\nu}-\frac{1}{12}(1-(R_{\mu\nu}+R_{\nu\mu})). \tag{2.21}$$

A more complete treatment was given by Lüsher and Weisz[22] where a set of Wilson loops were added to the plaquette with certain coefficients to cancel out the $O(a^2)$ error. One can refer to Fig. 2.2 for the set of Wilson loops.

Of course, there are other sets of Wilson loops one can add to the action so that the $O(a^2)$ correction is canceled among them. An example can be found in Snippe's square action[23]. The improvement generally facilitates the convergence as promised at much lower computational cost than brute-force reduction of the lattice size.

[3] A more pedagogical review can be found in [21]

2.4 Fermions on the Lattice

Transcription of the fermion sector of QCD on the lattice appears to be easier than the pure gauge action. However, naive regularization invokes some serious theoretical trouble which is deeply rooted in the chiral symmetry structure of QCD. In this section, quantization of fermions on the lattice and its issues will be described.

2.4.1 Wilson action

The fermionic sector of QCD is of the following form in Minkowski space:

$$L = \sum_f \bar{\psi}_f(x)(i\gamma^\mu D_\mu - m_f)\psi_f(x), \tag{2.22}$$

where $D_\mu \equiv \partial_\mu - igA_\mu(x)$. If we perform a Wick rotation and refer to our prescription 2.6, We will get:

$$L_M \rightarrow -\sum_f \bar{\psi}_f(x)(\gamma_E^i D_i + m_f)\psi_f(x) = -L_E, \tag{2.23}$$

where $D_i \equiv \partial_i + igA_i(x)$ and everything is defined in Euclidean space now. Euclidean γ matrices are defined:

$$\gamma_E^4 = \gamma_M^0 \qquad \gamma_E^i = i\gamma_M^i, \tag{2.24}$$

and they satisfy:

$$\{\gamma_E^i, \gamma_E^j\} = 2\delta_{i,j}, \tag{2.25}$$

where $i, j = 1 \ldots 4$. Now we have a Euclidean continuum QCD to compare our lattice action with.

A straight forward way to discretize L_E can easily be formulated:

$$\begin{aligned} L_q =& m_q\bar{\psi}(x)\psi(x) + \frac{1}{2a}\bar{\psi}(x)\sum_{i=1} 4\gamma_i \left(U_i(x)\psi(x+a\hat{i}) - U_i^\dagger(x-a\hat{i})\psi(x-a\hat{i})\right) \\ \equiv& \bar{\psi}(x)\sum_i(\gamma_i D_i + m_q)\psi(x). \end{aligned} \tag{2.26}$$

It is called the naive fermion action. The continuum covariant derivative is replaced by symmetric finite differences so that the lattice spacing error is reduced to $O(a^2)$. To demonstrate

this point, let's consider only the latter part of the action and expand the link as well as the ψ fields:

$$\begin{aligned} U_i(x) =& e^{-iagA_i(x+\frac{a}{2}\hat{i})} = 1 - iagA_i(x+\frac{a}{2}\hat{i}) + O(a^2), \\ U_i^\dagger(x) =& e^{iagA_i(x-\frac{a}{2}\hat{i})} = 1 + iagA_i(x-\frac{a}{2}\hat{i}) + O(a^2), \\ \psi(x+a\hat{i}) =& \psi(x) + a\partial_i(x) + O(a^2), \\ \psi(x-a\hat{i}) =& \psi(x) - a\partial_i(x) + O(a^2). \end{aligned} \tag{2.27}$$

After put all these pieces together we get:

$$\begin{aligned} L_q =& m_q\bar{\psi}(x)\psi(x) + \bar{\psi}(x)\sum_{i=1}^{4}\gamma_i\left(\partial_i + \frac{a^2}{6}\partial_i^3\right. \\ & \left. - ig(A_i + \frac{a^2}{2}(\frac{1}{4}\partial_i^2 A_i + (\partial_i A_i)\partial_i + A_i\partial_i^2))\right)\psi(x). \end{aligned} \tag{2.28}$$

It is clear that the lattice spacing error is of order a^2. In other words, the naive quark action has the comparable convergence as the Wilson gauge action 2.20.

However, a closer look at the action will reveal a serious problem. Consider the free field limit where $g = 0$, the action takes the following form:

$$\begin{aligned} S =& \sum_q\sum_{x,y}\bar{\psi}(x)\left(m_q\delta_{x,y} + \frac{1}{2a}\gamma_i(\delta_{x+a\hat{i},y} - \delta_{x-a\hat{i},y})\right)\psi(y) \\ =& \sum_q\sum_p\bar{\psi}(-p)\left(m_q + \frac{1}{a}\sum_{i=1}^{4}\gamma_i i\sin(p_i a)\right)\psi(p), \end{aligned} \tag{2.29}$$

where Fourier transformations to the momentum space were performed. It is easy to see that the momentum space quark propagator is:

$$P = \frac{-i\gamma_i\sin(p_i a) + m_q}{\sin^2(p_i a) + m_q^2}. \tag{2.30}$$

If we take $p_i = 0$ for $i = 1,2,3$, the on-shell condition will be:

$$\sin(p_4 a) = im_q. \tag{2.31}$$

However, for any p_4 that satisfies this relation, $\pi - p_4 a$ will satisfy this relation as well since we know $\sin(\alpha) = \sin(\pi - \alpha)$. The extra pole behaves like a particle which has no continuum counterpart but would not disappear as we simply take 2.26 to its continuum

limit. As a result, it is evident that for each dimension the number of "flavors" will double. In $d = 4$ Euclidean space we end up have $2^4 = 16$ species on the lattice for one single flavor in the continuum, which is impossible to simulate at present. This is the famous fermion doubling problem.

There is a straight forward way to cure the problem. Introduce the lattice Laplacian operator:

$$\Delta\psi(x) = \sum_{i=1} 4\left(U_i(x)\psi(x+\hat{i}) + U_i^{\dagger}(x-\hat{i})\psi(x-\hat{i}) - 2\psi(x)\right). \tag{2.32}$$

The operator is added to the naive quark action with an arbitrary coefficient r,

$$S_{W_q} = \sum_x \bar{\psi}(x) \sum_i (\gamma_i D_i - \frac{ar}{2}\Delta + m)\psi(x), \tag{2.33}$$

where D_i stands for the finite symmetric difference in 2.26. Now the denominator of the fermion propagator become:

$$\sin^2(p_4 a) + \left(ma + 2r\sin^2\left(\frac{p_4 a}{2}\right)\right). \tag{2.34}$$

Now the extra pole is damped away because of the presence of the $\sin^2\left(\frac{p_4 a}{2}\right)$ term. However, not only has an $O(a)$ error been introduced, but chiral symmetry present in continuum QCD has been broken leading to additive renormalization of quark mass. The inverse propagator is not protected against zero mass and might be singular even at finite quark mass.

After careful investigation, it turns out that the doubling problem has a much deeper physical reason for it. It was proven rigorously by Nielsen-Ninomiya[24] that doubling is inevitable if the following conditions are to be satisfied simultaneously[25]:

i. The fermion propagator is an *analytic periodic* function of the momenta p_i with period $2\pi/a$.

ii. For momenta much lower than cut-off, the continuum limit is valid up to order a^2p^2.

iii. The fermion propagator is non-singular for all non-zero(mod $2\pi/a$) momenta.

iv. The chiral symmetry of continuum QCD is respected exactly, i.e. γ_5 anti-commutes with inverse-fermion-propagator.

The first condition ensures the locality of the action while the second and the third guarantee the right continuum limit. The fourth one ensures that the lattice action bears *exactly* the same chiral symmetry as continuum QCD does. It is accepted that first three conditions are essential in order for a lattice action to be physically relevant. Therefore preservation of exact chiral symmetry and elimination of doublers seem to be mutually exclusive goals. The lattice community adopts two general approaches to the dilemma. The first one is to break chiral symmetry in favor of doubler free action, the Wilson action 2.33 is an example. The other approach is to preserve chiral symmetry at least to some extent. Staggered, domain wall and overlap fermions all belong to this category. It is this second approach that contributes the most to ongoing dynamical LQCD simulations.

2.4.2 Introduction to Staggered Fermions

The staggered fermion action was first introduced by J. B. Kogut and L. Susskind[26]. It is based on the so-called spin diagonalization technique. Let's recall the naive fermion action 2.26:

$$L_q = \bar{\psi}(x)(\sum_i \gamma_i D_i + m_q)\psi(x).$$

As was demonstrated before, the naive action has 16 distinct species quarks corresponding to each physical flavor. They are termed as different "tastes" of a single flavor so as not confuse the doublers with the desired physical quark flavors. In order to reduce the number of tastes if not completely eliminate them, it is observed that by performing a site-dependent bilinear transformation the kernel $\sum_i \gamma_i D_i$ can be diagonalized. Under the transformation we have:

$$\psi(x) = \gamma(x)\chi(x) \qquad \bar{\psi}(x) = \bar{\chi}(x)\gamma(x), \tag{2.35}$$

where:

$$\gamma(x) = \gamma_1^{x_1}\gamma_2^{x_2}\gamma_3^{x_3}\gamma_4^{x_4} \qquad \text{and} \qquad x = (x_1 a, x_2 a, x_3 a, x_4 a). \tag{2.36}$$

The naive quark action takes the following form:

$$S = \sum_x \sum_{\alpha=1}^{4} \bar{\chi}_\alpha(x) \left(\sum_i \eta_i(x) D_i + m \right) \chi_\alpha(x), \tag{2.37}$$

where $\eta_i(x) = (-1)^{x_1+\cdots+x_{i-1}}$ is a universal phase independent of spinor index α. Therefore the action contains exactly four degenerate replicas of a "staggered" field and it's legitimate

to drop the index α. By the above prescription the number of effective degrees of freedom decreases by a factor of 4 and the doubler problem is far less severe than it is in the naive action.

The staggered fermions also have another attracting property: remnant chiral symmetry. Consider the massless limit of the staggered quark action:

$$S = \sum_x \sum_i \bar{\chi}_\alpha(x)\eta_i(x)D_i\chi(x). \tag{2.38}$$

It can be shown that such an action is invariant under $U(4)_L \otimes U(4)_R = U(1)_V \otimes U(1)_A \otimes SU(4)_L \otimes SU(4)_R$. Although the chiral symmetry present in the staggered quark action is much less powerful than the counterpart in continuum QCD, it is nevertheless good enough to prevent additive mass renormalization and therefore not only protects the inverse propagator from exceptional singular modes but also facilitates chiral extrapolation down to the physical mass region[4].

Furthermore, the staggered quark is cheaper to simulate. All these virtues combine together to make the staggered quark action a good candidate for dynamical simulation. Nowadays the action used is usually $O(a^2)$ improved. Together with other techniques such as tadpole improvement[27] and the $O(a^2)$ improved gauge action, the improved staggered quark action makes LQCD calculation relevant to phenomenological quantities for the first time.

However, the staggered quark action does have its own drawbacks[28]. First of all, spin and taste degrees of freedom conspire in a subtle way in order for the staggered quark action to work. For each flavor in the real physical world there are 4 degenerate staggered flavors on a sublattice with lattice spacing $2a$ thanks to the $2a$ periodicity of $\eta(x)$. Inside the $2a$ hyper-cube the degeneracy is lifted and 16 degrees of freedoms which are a mixture of spin and taste degrees of freedoms are present. Therefore it is highly non-trivial to construct and interpret operators in terms of spin and flavor, which makes the action non-user-friendly and non-intuitive to some extent. Due to this drawback, the Wilson quark action has been frequently used, though its great computational cost has been an impediment to its use in realistic unquenched simulations.

Second of all, the action is not actually doubler free and there are still 4 staggered flavors for each "input flavor" which is still too many for real dynamical simulation. A further trick,

[4]The necessity of the extrapolation will be discussed in Section 2.5.

the so-called root trick[29], is introduced to reduce number of degrees of freedom one more step. The theoretical legitimacy and conceptual validity of the trick is still under debate. However, various evidences from different approaches including perturbation theory, RG arguments and effective field theory arguments suggest that the rooted staggered quark does converge to QCD in the continuum limit[30].

2.4.3 Further effort on a satisfactory fermionic action

While lattice theorists are trying to improve Wilson action and understand more about the root trick of the staggered quark, tremendous efforts have been made in order to develop other good lattice fermion actions. Although all actions present today suffer from either conceptual unclearness or practical infeasibility, great improvements have nevertheless been made. A brief survey will be given in this section of major actions in the field.

Firstly, a new algorithm invented by Lüscher[31] made unquenched simulations using Wilson quarks possible. As was discussed in Section 2.4, Wilson quarks have been long troubled by the critical slowing-down problem in exceptional gauge field configurations in which light quarks are essentially massless. The so-called domain-decomposition method divides a finite lattice into small blocks whose sizes are no more than 1 fm. Interactions between distant blocks are considered to be weak. Generally different blocks are first decoupled completely and interactions between blocks are treated as corrections. Combined with the Hybrid Monte Carlo algorithm[32], the domain-decomposition algorithm shows some encouraging results[33].

The second approach is twisted mass LQCD(tmLQCD)[34]. Initially proposed as a tool to study spontaneous parity and flavor symmetry breaking, tmLQCD as an alternative regularization of QCD has been an interesting subject of the lattice community for several years. In its simplest version containing one flavor doublet the tmLQCD action reads:

$$\begin{aligned} S &= S_g[U] + S_F[U,\psi,\bar{\psi}] \\ &= S_g[U] + a^4 \sum_x \{\bar{\psi}(x)\left(D[U] + m_0 + i\mu\gamma_5\tau^3\right)\psi(x)\}. \end{aligned} \tag{2.39}$$

τ^3 is the third Pauli matrix. m_0 is the bare mass term while μ is the twisted mass. $D[U]$ is the kernel of the Wilson action 2.33 without the mass term. It was shown that the inverse propagator of tmLQCD action is protected from the zero mode by finite μ despite chiral

symmetry being broken by a Wilson term. For particular choices of μ, the action is automatically $O(a)$ improved. Furthermore, the action's computational cost is almost as cheap as the staggered quark action. However, the action does break flavor and parity symmetries that will be only recovered in the continuum limit, which causes unwanted splitting between physically degenerate states. This issue is being addressed with dynamical simulations. All in all, tmLQCD has many attractive properties and would provide an alternative for dynamical simulations if on-going investigations of the action yield positive results.

The third approach is the perfect action pioneered by Hasenfratz and Niedermayer[35]. Based on the renormalization group method, it is hoped that cut-off effects can be eliminated from lattice simulation no matter what the lattice spacing is. Fermion fields on lattice are obtained through block averaging continuum fields. The resulting lattice action should in principle be equivalent to continuum QCD. The perfect action was proven to obey the Ginsparg-Wilson relation which is thought to be the correct definition of chiral symmetry on lattice non-perturbatively. However, it is practically not possible to solve the analytical form of the perfect fermion action and thus the actual simulations rely on a complicated process to fit the RG equations. Therefore the perfect action is too expensive to simulate despite its theoretical appeal.

The fourth approach is domain wall fermions proposed by David B. Kaplan[36] in 1992. It is a 5-dimensional model related to similar ideas in the continuum. In this prescription, massless chiral fermions are confined in the kink present in the 5th dimension to separate regions of opposite masses. It is then observed that once boundary conditions are imposed on a finite 5th dimension, an anti-wall will appear with chiral fermions of opposite chirality of the original wall confined in it. Two walls are separated and their overlap decreases exponentially as the distance between them increases. If the distance is taken to be infinity, we obtain the so-called overlap fermion developed independently by Narayanan and Neuberger[37]. which obeys Ginsparg-Wilson relation exactly. Despite the interesting chiral properties and some early attempts to use these actions in unquenched simulations, they are both fairly expensive to simulate dynamically.

2.5 Complete Lattice QCD

In previous Sections different ways of transcribing gauge boson and fermion degrees of freedom on a lattice were reviewed. A lattice version of full QCD can be obtained by addition of a gauge action and a consistent quark action, for example, sum of the Wilson gauge action 2.20 and the Wilson quark action 2.33:

$$S_{QCD} = S_g + S_q.$$

Generically, the fermion action can be write as the following form:

$$S_q = \sum_{x,y} \bar{\psi}_i(x) M_{i,x;j,y} \psi_j(y), \tag{2.40}$$

where i, j denote flavor and other relevant quantum numbers. As was discussed in Section 2.1, the expectation value of a general operator O can be calculated by averaging it over different field configurations. Fermion fields would be described with Grassmann numbers on lattice. However, since these numbers are hard to implement numerically, fermionic part of path integrals are performed analytically thanks to the quadratic form of fermion action:

$$Z = \int DA_i det(M) e^{-S_g}. \tag{2.41}$$

We can then write the action in terms of pure gauge fields despite M being highly non-local:

$$S = S_g - \sum_i \log(Det M_i). \tag{2.42}$$

It is also important to have a gauge invariant integration measure for gluon fields. The measure is defined in terms of the same link variables as those used in the action. Link fields are unitary matrices with determinant 1. It is proposed by Wilson to introduce an invariant $SU(3)$ group measure, the Haar measure, as the integration measure. The measure is normalized to be 1:

$$\int dU = 1. \tag{2.43}$$

Given that U_1 and U_2 are arbitrary $SU(3)$ elements and that $f(U)$ is a function of U, the measure satisfies:

$$\int dU f(U) = \int dU f(UU_1) = \int dU f(U_2 U). \tag{2.44}$$

Once the action is picked, different background gauge field configurations are generated in actual simulation. Although the number of field configurations is infinite, the probability distribution is peaked around the field configuration which minimizes the free energy. Configurations around the peak dominate the functional integral. Therefore they should be generated with higher priority.

After background gauge field configurations are generated, the quark propagator should be calculated by inverting M. In an unquenched simulation, the inversion of M is performed in each step of the Monte-Carlo simulation as well. The inversion of M consumes most of the time of a lattice calculation. Naturally it is the bottleneck of lattice action in several ways. First of all, the size of M will increase dramatically as the number of lattice sites and number of quark species increase. Together with the finite lattice volume in order to accommodate a system of interest, a practical upper bound of lattice site number severely constrains the lower limit of the lattice spacing. Furthermore, if we are working at physical up or down quark mass, inversion of M will be extremely expensive since the matrix will have almost zero eigenvalues. This is the so called critical slowing-down problem. Practically people work with higher light quark mass and then extrapolate the results to the physical light quark mass. This is the practical reason why the lattice community tried so hard to construct the chiral symmetric and doubler free action.

In the final step, the operator of interest is averaged over different configurations.

For a long time the lattice community had to impose the so-called "quenched" approximation due to the limitation of computer power and lack of relevant techniques. Under this approximation one declares $det(M) = 1$ in 2.42. Physically, such an approximation eliminates all the sea quark effects in lattice calculation. The quenched approximation made many important contributions including evidence for confinement and chiral symmetry breaking on the lattice. However, this is not really an approximation, since one has no systematic control over the errors which are thereby introduced. If lattice calculations are to be relevant to phenomenology whether for comparison or for prediction, the quenched approximation must be lifted and dynamical quarks have to be introduced.

2.6 Lattice Perturbation Theory

In previous sections I have been advocating that the lattice is one of the most effective tools to explore the non-perturbative aspect of QCD. Indeed, the simulation process introduced in Section 2.5 is essentially non-perturbative. It's somewhat ironic to talk about Lattice Perturbation Theory(LPT)[38] right after all that I said. However, LPT is very important if not indispensable in order for Monte-Carlo simulation results to have any physical meaning for reasons which will be clear after the current section.

Before motivating the importance of LPT, it is appropriate to give a description of what LPT is. For a specific lattice action, say the Wilson action, we can Taylor-expand all the link variables:

$$\begin{aligned} U_\mu(x) =& e^{igaA_\mu(x+\frac{\mu}{2})} \\ =& 1+igaA_\mu(x+\frac{\mu}{2})-\frac{1}{2}g^2a^2A_\mu^2(x+\frac{\mu}{2})+\ldots. \end{aligned} \tag{2.45}$$

Here g can be seen as the bare coupling which is defined at cut-off scale $\frac{\pi}{a}$. Generally we have a relatively small lattice spacing so that the cut off scale is larger than Λ_{QCD} so we expect the relevant $\alpha_s < 1$. Therefore after Taylor expanding the link fields, the lattice action will have the form of free field part plus a tower of different interactions organized in powers of a and g, just like a non-renormalizable continuum quantum field theory. It is useful to view such a theory as a effective field theory. Although an exact solution is impossible, the theory does possess predictive power up to a certain accuracy by keeping interaction terms to a corresponding order of a and g. After truncating the action to the order, perturbation theory can be used to calculate matrix elements and correlation functions. It is worth noticing that the truncated action should be gauge invariant if the truncation is done consistently, since the original action is gauge invariant. A more detailed description of LPT will be presented in the next chapter.

With this simple description in mind we are able to appreciate the importance of LPT now. It can be seen from two perspectives.

First of all, LPT is needed in many cases to explain Monte-Carlo simulation results. A generic quantum field theory calculation must first introduce a regularization scheme in order for it to yield a finite result. Then the result has to be renormalized by eliminating the regularization scale through a proper renormalization process. For example, in dimensional

regularization we introduce cut-off Λ so that the logarithmic infinity is rendered to be $\ln(\frac{\Lambda}{p})$, then we introduce the $\overline{MS}$ scheme so that the cut-off is eliminated by subtracting off $\ln(\frac{\Lambda}{\mu})$ and some constants from the result. On the lattice we have a similar process. Lattice can be viewed as a non-perturbative *regularization* scale $\frac{\pi}{a}$. Somehow the regularization scale should be sent to infinity or equivalently a should go to 0 to yield a physically meaningful result. In the ideal world the renormalization part can be done by simulating at finer and finer lattice spacing a so that an extrapolation to $a = 0$ can be done literally. Unfortunately it is not feasible given computer power today. It is therefore up to LPT to map the lattice renormalization scheme(notice now within LPT renormalization is done *perturbatively*) to a continuum renormalization scheme, say the $\overline{MS}$ scheme, so that they yield the same result for various matrix elements. Since I am not doing any matching calculations here, interested readers can refer to corresponding sections in [38].

I should mention that renormalization can also be done non-perturbatively using the Schrödinger functional in some cases. However, it's generally more expensive to compute and its result agree with LPT results providing that proper schemes are chosen for LPT.

Second of all, LPT is one of the primary tools to improve the convergence of lattice actions. As was discussed in Section 2.3.2, convergence of lattice actions can be improved by adding new gauge invariant terms with coefficients designed to cancel errors to certain orders in the lattice spacing a. We also have discussed that a lattice action in LPT expansions can be regarded as an effective field theory. It is expected that all the quantities related to it will receive quantum corrections from loop diagrams. For example, the scaling violations will be of order $O(\alpha_s^m a^n)$ as well as $O(a^n)$. Given the coarse lattice size we are limited to nowadays, α_s is roughly of order 0.1. Therefore if we want to keep our theoretical systematic error under $O(a^2)$ for, say, Wilson fermions, not only the $O(a)$ error but also the $O(\alpha_s a)$ error should be removed. It is only possible with the aid of LPT.

Given the relevance of LPT to interpreting the simulation results and to improving the scaling properties, it is necessary for us to understand its drawbacks and ways to deal with these drawbacks. Since symmetry constraints on lattice is milder than continuum, the allowed interaction terms are generally more complicated. To make the situation worse, different lattice actions give rise to very distinct sets of Feynman rules, which require separate treatments. However, as we will see in the next chapter in more detail, an algorithm invented by Lüscher and Weisz[12] makes it possible to automate the generation of Feynman

rules for almost arbitrary lattice actions. Combining with other techniques such as tadpole improvement[27], LPT contributes greatly to the on-going dynamical simulation quest.

2.7 Sources of theoretical errors

In the last section of the chapter, I will summarize simply different possible sources of lattice errors. A more detailed account can be found in [39].

First of all, statistical errors are introduced by Monte-carlo simulations. Generally such errors will fall as $1/\sqrt{N}$ where N is the number of independent measurements. Given the large number of configurations available today, statistical errors are often small in comparison with theoretical systematic errors.

The second source is comprised of finite lattice spacing errors. This source has been the subject of discussion in previous sections and it is also my primary target of improvement here.

Finite volume errors comprise the third source. In order for actual numerical simulation to be feasible, not only does continuum space-time have to be discretized but the lattice also has to be confined into a finite volume so that the number of degrees of freedom is rendered finite. Such errors manifest themselves in two ways. Firstly, by imposing periodic boundary conditions the actual simulated system can be regarded as infinite space filled with periodic cells and there is a identical copy of the system of interest, say a proton, in each cell. Naturally these copies are expected to interact with each other. One can parameterize the interaction with a Yukawa like coupling and it is estimated[40] that for sufficiently large lattice side length L the finite volume error caused by the interaction falls as e^{-ML}/L where M is the mass of the system of interest. It is therefore preferred to adopt a L large enough so that the error due to interactions falls exponentially. Secondly, L decides the resolution of the lattice momentum sum. The lowest momentum mode is $\frac{2\pi}{La}$ under periodic boundary conditions. In order to increase resolution, L or a should be increased. This aspect also ties to the finite lattice spacing error in the sense that if we want to keep the number of degrees of freedom stable and increase resolution L and a must be increased simultaneously, implying larger finite lattice spacing errors.

A major source of uncontrollable systematic errors comes from quenched approximation. With introduction of dynamical fermions it is no longer a problem. There are also

other sources of errors such as errors coming from chiral extrapolation, renormalization factors, operator mixing, etc. Efforts to control all of them are necessary in order for LQCD to be relevant to phenomenology.

Chapter 3

A review of important techniques

Two important techniques will be reviewed in detail in this chapter. First of all, Lattice Perturbation Theory(LPT) will be described in detail for both the gauge action and the fermion action. The algorithm developed by Lüscher and Weisz will be introduced. After that, the other important technique, namely twisted periodic boundary conditions will be reviewed.

3.1 Lattice Perturbation Theory

LPT was briefly sketched and motivated in Section 2.6. Given its essential status for my work here, it is necessary to review it in greater detail. The review here is based on [38].

3.1.1 Pure gauge action and Fermion action

The expansion of the pure gauge action in non-Abelian theory is greatly complicated by the non-commutivity of link fields even for a plaquette. One can get a taste of the difficulty by deriving the lowest order gauge action[1]. According to the Baker-Campbell-Hausdorff relation we have:

$$e^A e^B = exp\{A+B+\frac{1}{2}[A,B]+\ldots\}. \tag{3.1}$$

[1]The derivation here is the $SU(3)$ version of the corresponding part in Kogut's review[41].

Let's denote the plaquette in the following form:

$$e^A e^B e^C e^D$$

with

$$A \equiv iagA_\mu(x_0 - \frac{a}{2}\hat{\nu}) \qquad C \equiv iagA_\mu(x_0 + \frac{a}{2}\hat{\nu})$$
$$\text{and}$$
$$B \equiv iagA_\nu(x_0 + \frac{a}{2}\hat{\mu}), \qquad D \equiv iagA_\mu(x_0 - \frac{a}{2}\hat{\mu}),$$

where $x_0 \equiv x + \frac{a}{2}\hat{\mu} + \frac{a}{2}\hat{\nu}$. Now we have:

$$\begin{aligned} e^A e^B e^C e^D &= \exp\{A+B+\frac{1}{2}[A,B]\}\exp\{C+D+\frac{1}{2}[C,D]\} \\ &= \exp\{A+B+C+D+\frac{1}{2}([A,B]+[C,D]+[A,C]+[B,D]+[A,D]+[B,C])\} \\ &\simeq \exp\{ia^2 g(\partial_\mu A_\nu - \partial_\nu A_\mu + ig[A_\mu, A_\nu])\} \\ &= \exp\{ia^2 g F_{\mu\nu}\}, \end{aligned}$$

where we define $a\partial_\mu A_\nu(x_0) \equiv A_\nu(x_0 + \frac{a}{2}\hat{\mu}) - A_\nu(x_0 + \frac{a}{2}\hat{\nu})$. Notice the final result is the same as 3.1.1 for the Abelian case. The gluon propagator can not be determined at the moment due to contributions from the integration measure and gauge fixing terms. The expansion will also produce a tower of different interaction vertices with different numbers of gluons. Even the lowest order interaction vertex is more complicated than in the continuum with lattice artifacts of higher order in a.

The complete form of the 3-gluon vertex for the plaquette action is given in [38]:

$$\begin{aligned} W^{abc}_{\mu\nu\lambda}(p,q,r) = &-ig_0 f^{abc}\frac{2}{a}\{\delta_{\mu\nu}\sin\frac{a(p-q)_\lambda}{2}\cos\frac{ar_\mu}{2} \\ &+\delta_{\nu\lambda}\sin\frac{a(q-r)_\mu}{2}\cos\frac{ap_\nu}{2} + \delta_{\mu\lambda}\sin\frac{a(r-p)_\nu}{2}\cos\frac{aq_\lambda}{2}\}, \end{aligned} \tag{3.2}$$

where $p+q+r=0$ and all momenta are flowing into the vertex. It can be seen that as $a \to 0$, 3.2 will converge to its continuum form. However, all the lattice artifacts are necessary to ensure local gauge invariance. Despite the relatively simple form of the 3-gluon vertex, higher order vertices will be very tedious to write down. For the explicit form of 4-gluon vertex one can refer to [38]. Moreover, for an improved gluon action even 3-gluon vertex will be much more complicated. Lüscher and Weisz[12] gave an estimate of the number of terms in a typical vertex of r gluons:

$$n_{r,l} = \frac{2}{(r-1)!}l(l+1)\cdots(l+r-1), \tag{3.3}$$

where l is the circumference of the Wilson loop in the relevant Lattice Gauge action. Nowadays people typically use order a^2 improved actions which imply $l = 6$. If we consider $r = 6$, we will have 5544 terms in the vertex function. The above example gives a sense of the complexity of the problem we are dealing with.

LPT for the fermion action can be visualized in a straightforward way. After link variables are Taylor-expanded, it is clear that there will be a tower of couplings between quarks and two or more gluons in addition to the minimal coupling in the continuum.

3.1.2 Contributions from the measure

It was discussed in Section 2.1 that the integration measure of the link fields is defined as the invariant Haar measure of $SU(3)$ group. However, the proper degrees of freedom for perturbation theory are the gauge field $A_\mu(x)$. Therefore a relation between the integration measures we used for link field and DA needs to be established. Consider the following two form:

$$d^2s = Tr(dU_\mu^\dagger dU_\mu), \tag{3.4}$$

where $dU(x) \equiv dU_\mu(A_\mu + dA_\mu) - dU(A_\mu)$ and dA_μ is the gauge-field integration element. It is clear that 3.4 is invariant under local gauge transformations. If we write d^2s in terms of vector gauge potential A_μ in the perturbative region, a measure g can be introduced:

$$d^2s = g_{ab}(A) dA_\mu^a dA_\mu^b. \tag{3.5}$$

Therefore the gauge invariant Haar measure is defined to be:

$$d\mu(A) = \prod_{x,a} \sqrt{\det g(A)} dA_\mu^a. \tag{3.6}$$

$g(A)$ is only dependent on the properties of $SU(3)$ group.

Following the road map described above, we need to first express the two form in terms of A_μ. It was derived[42] that a link field with an infinitesimal change of A_μ can be expanded as follows:

$$U_\mu(A_\mu + dA_\mu) = U_\mu(A_\mu)(1 + iagdA_\mu^a M_{ab}(A_\mu) T^b), \tag{3.7}$$

where repeated color indices a, b imply summation. $M_{ab}(A_\mu)$ is a matrix. It is the unit matrix in the continuum limit. For finite lattice spacing, it is defined as follows:

$$M(A_\mu) = \frac{e^{iagA^a t^a} - 1}{iagA^a t^a}, \tag{3.8}$$

where $(t^a)^{bc} = -if^{abc}$.

Now we are ready to derive the explicit form of 3.4:

$$\begin{aligned} d^2s =& Tr(dU_\mu^\dagger dU_\mu) \\ =& Tr\{-iT^c M_{ca}^\dagger(A_\mu) agdA_\mu^a U_\mu^\dagger(A_\mu) U_\mu(A_\mu) iagdA_\mu^b M_{bd}(A_\mu) T^d\} \\ =& a^2g^2\frac{1}{2}\delta^{cd} M_{ca}^\dagger(A_\mu) M_{bd}(A_\mu) dA_\mu^a dA_\mu^b \\ =& \frac{1}{2}a^2g^2 M_{ca}^\dagger(A_\mu) M_{bc}(A_\mu) dA_\mu^a dA_\mu^b, \end{aligned} \tag{3.9}$$

where we used relation $Tr(T^cT^d) = \frac{1}{2}\delta^{cd}$. Combining the result of 3.9 with 3.5 we get the expression for $g(A)$:

$$\begin{aligned} g(A) =& \frac{1}{2}\left(M^\dagger(A)M(A)\right) \\ =& \frac{1}{2}\cdot\frac{2 - e^{iagA^at^a} - e^{-iagA^at^a}}{(agA_\mu^at^a)^2} \\ =& \frac{1-\cos(agA^at^a)}{(agA_\mu^at^a)^2} \\ =& \frac{1}{2} + \sum_{n=1}^{\infty}\frac{(-1)^n}{(2n+2)!}(iagA_\mu^at^a)^{2n}. \end{aligned} \tag{3.10}$$

Now we are ready to derive the explicit form of the Haar measure defined in 3.6. If we define $DA = \prod_{x,\mu,a} dA_\mu^a(x)$, the Haar measure can be expressed as follows:

$$d\mu(A) \equiv DU = \prod_{x,\mu}\sqrt{\det(g(A))} = e^{-S_{measure}(A)}DA. \tag{3.11}$$

Using the relation $\det g = exp(Tr\log g)$ $S_{measure}(A)$ can be expressed as follows:

$$S_{measure}(A) = -\frac{1}{2}\sum_{x,\mu} Tr\log\left(1 + 2\sum_{n=1}^{\infty}\frac{(-1)^n}{(2n+2)!}(iagA_\mu^at^a)^{2n}\right). \tag{3.12}$$

It is evident that the integration measure over $A_\mu^a(x)$ contains a tower of interaction terms non-trivially. It is also clear that the interaction terms are the result of the non-Abelian nature of the $SU(3)$ group. For an Abelian group $(t^a)^{bc} = -if^{abc} = 0$, we would have $DU = DA$.

The lowest order interaction term is a "two gluon" vertex. Using the relation $Tr(t^a t^b) = 3\delta^{ab}$ it can be derived that to the lowest order of g:

$$S_{measure}(A) = \frac{g^2}{8a^2} \sum_{x,a,\mu} (A^a_\mu)^2. \tag{3.13}$$

Therefore these interactions will not contribute to tree level processes.

3.1.3 Faddeev-Popov gauge fixing

Gauge fixing is an important step in order for any continuum gauge theory to produce physical predictions. Field configurations differing by a gauge transformation will produce identical physical observables and thus describe the same universe. Intuitively, we can imagine there are infinite copies of our universe on the gauge potential level each of which will contribute the same amount to the path-integral and lead to an inevitable un-physical divergence. In order to fix the problem, we need to fix our description to a particular gauge so that only one copy of universe is left at the cost of losing manifest gauge invariance.

For LQCD we generally don't have to fix the gauge since the volume of the phase space of U_μ is finite. However, degrees of freedom shift back to A_μ in LPT once we expand all the link fields. A proper gauge fixing process is therefore needed to free us from a divergent path-integral. As in the continuum, the goal can be achieved with the aid of the Faddeev-Popov method.

One can refer to [16] for gauge fixing in continuum QFT. The Faddeev-Popov method proceeds in essentially the same way on the lattice. First, the gauge fixing condition is chosen to be:

$$F^a_x[A, \omega] = \partial_\mu A^a_\mu(x) - \omega^a(x) = 0, \tag{3.14}$$

where $\partial_\mu \equiv \frac{1}{a}\left(\delta_{x,x+\frac{a}{2}\hat{\mu}} - \delta_{x,x-\frac{a}{2}\hat{\mu}}\right)$. As in the continuum we can introduce Faddeev-Popov determinant $\Delta_{FP}[A^\alpha, \omega]$ using the following relation:

$$\int D\alpha \delta\left(F[A^\alpha, \omega]\right) \Delta_{FP}[A^\alpha, \omega] = 1, \tag{3.15}$$

where α is a gauge transformation function and A^α is the gauge potential after the gauge transformation. We can now insert 3.15 into the path integral:

$$\int DA \int D\alpha \delta\left(F[A^\alpha, \omega]\right) \Delta_{FP}[A^\alpha, \omega] e^{-S_{QCD} - S_{measure}}.$$

Then we integrate over ω^a with a gaussian weight:

$$\begin{aligned}&\int DA \int D\alpha \int D\omega\delta(F[A^\alpha,\omega])\,\Delta_{FP}[A^\alpha,\omega]e^{-S_{QCD}-S_{measure}}e^{-\frac{1}{2\xi}a^4\sum_{x,a}\omega^a(x)\omega^a(x)}\\ =&\int DAD\alpha\Delta_{FP}[A^\alpha,\omega]e^{-S_{QCD}-S_{measure}-\frac{a^4}{2\xi}\sum_{x,a}(\partial_\mu A^a_\mu(x))^2},\end{aligned} \tag{3.16}$$

where the integration over $\omega^a(x)$ was completed with the aid of the delta function. It is now clear that there are two effects of Faddeev-Popov gauge fixing. Firstly, an extra term $S_{gf} \equiv \frac{a^4}{2\xi}\sum_{x,a}(\partial_\mu A^a_\mu(x))^2$ is added to the action; the other effect is the Faddeev-Popov determinant which will give rise to interaction with ghost fields as in the continuum.

Let's consider S_{gf} first:

$$\begin{aligned}S_{gf} =&\frac{a^4}{2\xi}\sum_{x,a}(\partial_\mu A^a_\mu(x))^2 = \frac{a^2}{2\xi}(A^a_\mu(x+\frac{a}{2}\hat{\mu})-A^a_\mu(x-\frac{a}{2}\hat{\mu}))\\ =&\frac{a^3}{2\xi}\sum_{x,a}\left(A^a_\mu(x+\frac{a}{2}\hat{\mu})\partial_\nu A^a_\nu(x)-A^a_\mu(x-\frac{a}{2}\hat{\mu})\partial_\nu A^a_\mu(x)\right)^2\\ =&\frac{a^3}{2\xi}\sum_{x,a}\left(A^a_\mu(x)\partial_\nu A^a_\nu(x-\frac{a}{2}\hat{\mu})-A^a_\mu(x)\partial_\nu A^a_\nu(x+\frac{a}{2}\hat{\mu})\right)\\ =&-\frac{a^4}{2\xi}\sum_{x,a}A^a_\mu(x)\partial_\nu\partial_\mu A^a_\nu(x).\end{aligned} \tag{3.17}$$

It can also be seen as an illustration that integrating by parts works for a finite lattice sum as well as long as we have translational invariance. Let's recall the unimproved Wilson gauge action in S_{QCD} in 3.1.1:

$$\begin{aligned}S_g =&\frac{a^4}{4}\sum_{x,a}(\partial_\mu A^a_\nu-\partial_\nu A^a_\mu)^2\\ =&\frac{a^4}{2}\sum_{x,a}(\partial_\mu A^a_\nu\partial_\mu A^a_\nu-\partial_\mu A^a_\nu\partial_\nu A^a_\mu)\\ =&-\frac{a^4}{2}\sum_{x,a}A^a_\nu(\partial_\mu\partial_\nu\delta_{\mu\nu}-\partial_\nu\partial_\mu)A^a_\mu.\end{aligned} \tag{3.18}$$

In momentum space, S_g+S_{gf} reads for infinite lattice:

$$\begin{aligned}&S_g+S_{gf}\\ =&\int\frac{d^4k}{(2\pi)^4}A^a_\mu(k)\left(4\sin^2(\frac{ak_\mu}{2})-4(1-\frac{1}{\xi})\sin(\frac{ak_\mu}{2})\sin(\frac{ak_\nu}{2})\right)A^a_\nu(k),\end{aligned} \tag{3.19}$$

where the integration over each component of k is limited to the first Brillouin zone $[-\frac{\pi}{a}, \frac{\pi}{a}]$. For a finite lattice, the integration will be replaced by a finite sum while the kernel remains the same. Therefore the full propagator for the particular action and gauge fixing condition is:

$$G^{ab}_{\mu\nu} = \frac{\delta^{ab}}{\frac{4}{a^2}\sum_\rho \sin^2\frac{ak_\rho}{2}}\left(\delta_{\mu\nu} - (1-\xi)\frac{\sin\frac{k_\mu}{2}\sin\frac{k_\nu}{2}}{\sum_\rho \sin^2\frac{ak_\rho}{2}}\right). \tag{3.20}$$

The continuum limit of the action is consistent with the gluon propagator obtained using the compatible gauge fixing condition. By setting $\xi = 1$ we will recover the familiar Feynman gauge. I should mention that generally an improved action will produce a gluon propagator with spin-indices not diagonalized. The spin diagonalization for the Feynman gauge in the case of an unimproved Wilson action is merely an accident.

Similarly to continuum QCD, the lattice Faddeev-Popov determinant will give rise to interactions with ghost fields. First we need to write out the explicit form of the Faddeev-Popov determinant. In order to do that, we need to make use of 3.7 in more general forms. For simplicity the lattice spacing a and the strong coupling g will be set to be 1 temporarily:

$$\begin{aligned} U(A_\mu + dA_\mu) =& U(A_\mu)(1 + dA^a_\mu M_{ab}(A)T^b) \\ =& (1 + dA^a_\mu M_{ab}(-A)T^b)U(A_\mu). \end{aligned} \tag{3.21}$$

Their derivations can be found in [42]. In analogy to continuum QCD, the Faddeev-Popov determinant is the linear response to an infinitesimal gauge transformation. Explicitly we have:

$$e^{i\varepsilon^a(x)T^a}U_\mu(A_\mu)e^{-i\varepsilon^a(x+\hat{\mu})T^a} = U_\mu(A_{mu} + \delta_\varepsilon A_\mu) \tag{3.22}$$

and we need to identify δ_ε.

Then we need to make use of 3.21. The infinitesimal gauge transformation can be performed through two steps. First $e^{-i\varepsilon^a(x+\hat{\mu})T^a}$ is multiplied to the left side of U_μ. We have:

$$\begin{aligned} U_\mu(A_\mu)e^{-i\varepsilon^a(x+\hat{\mu})T^a} =& U(A_\mu + \delta^L_\varepsilon A_\mu) \\ =& U(A_\mu)(1 + \delta^L_\varepsilon A^a_\mu M_{ab}(A)T^b). \end{aligned} \tag{3.23}$$

We can also get a first order expression by expanding $e^{-i\varepsilon^a(x+\hat{\mu})T^a} = 1 - i\varepsilon^a(x+\hat{\mu})T^a$. Combining the two expressions together, it can be solved that:

$$\delta^L_\varepsilon A^a_\mu = -M^{-1}_{ab}(A)\varepsilon^b. \tag{3.24}$$

Keeping only the linear term, we can get the second part of $\delta_\varepsilon A_\mu$:

$$\delta^R_\varepsilon A^a_\mu = M^{-1}_{ab}(-A)\varepsilon^b. \tag{3.25}$$

Recall the explicit form for $M_{ab}(A)$ in 3.8 and combine the two parts together:

$$\delta_\varepsilon A^a_\mu = -(iA^c_\mu t^c + M^{-1}(A)\partial^R_\mu)_{ab}\varepsilon^b(x), \tag{3.26}$$

where t^c is the $SU(3)$ generator in the adjoint representation and $\partial^R_\mu \equiv \delta^{x,x+\hat{\mu}} - 1$. Now we can establish the explicit form of the Faddeev-Popov determinant with a and g restored:

$$\begin{aligned}\Delta_{FP}[A] =& \det(-\partial_\mu D_\mu[A]) \\ =& \det(-\partial_\mu(M^{-1}(A)\cdot\partial^R_\mu + iagA^a_\mu(x)t^a)).\end{aligned} \tag{3.27}$$

We can introduce ghost fields c and $\bar{c}$ so that the determinant can be reexpressed as a Lagrangian involving ghost fields and their interactions with gauge field:

$$S_{gh} = a^4 \sum_{x,i,j} \bar{c}_i(\partial_\mu D_\mu[A])c_j, \tag{3.28}$$

which does have the correct continuum limit. However, the presence of $M^{-1}(A)$ gives rise to a tower of interactions of different numbers of gluons coupling with ghost fields. As in other sectors, the perturbation theory on the lattice for ghost field is much more cumbersome than in the continuum.

3.2 The automatic generation of LPT Feynman rules

Given the formidable complexity of LPT, errors can come into calculations in almost all stages of a conventional scenario of application of perturbation theory. First of all, it is hard to make no mistake in deriving Feynman rules for a particular lattice action. Even if one succeeded in Feynman rule derivation, the intrinsic nonlinearity of the lattice formalism and the complicated structure of vertices intimidates, if not prevents, any analytical attempt to perform a loop calculation. To make matters worse, different lattice actions are employed either to study different physical systems in order to take maximum advantage of their specific physical features or to simulate one single system so that comparisons among the actions can serve as tests for certain theoretical ideas. While these actions share the same

continuum limit as they should, the relatively weak symmetry constraints on the lattice allow them to differ greatly in lattice artifacts and therefore result in quite different vertex structures. If one wants to make use of different actions to attack phenomenologically relevant problems, analytical study of all of them is a totally unnecessary burden. Given all the arguments above, it is necessary or even essential for us to be able to generate Feynman rules especially vertex functions automatically for a generic lattice action.

Fortunately, such an algorithm already exists thanks to Lüscher and Weisz's pioneering work[12]. Since the algorithm is essential for my current work, a detailed description of it in a separate section is appropriate. The author also wants to state that the Feynman rules used for his calculation are provided by Dr. Howard D. Trottier who implemented the algorithm of [12]. The description here is based on Matthew Nobes' perspective[21]. One can refer to the original paper by Lüscher and Weisz[12] and other references[43][44] if a different understanding is needed for his/her research.

3.2.1 Lüscher and Weisz's algorithm: pure gauge action

As discussed before, our goal is to generate vertex functions automatically for a generic lattice action. An effective field theory point of view can be adopted for phenomenological purposes so that only interactions to a certain order of strong coupling g will be kept.

From the discussion in Chapter 2 we know that a general local gauge invariant lattice action is the summation of Wilson loops and Wilson lines of different sizes. In particular a pure gauge action is a summation of Wilson loops:

$$S_g = \sum_C \sum_x ReTr(1-C) = \sum_C S(C), \tag{3.29}$$

where C denotes a Wilson loop of a specific shape and $S(C) \equiv \sum_x ReTr(1-C)$. For a naive Wilson action the C's are plaquettes of different directions. Now, we need to generate vertex functions for a sub-action $S(C)$ where C is of arbitrary shape.

First of all, it will be helpful if the problem is defined more explicitly. A particular sub-action is defined by the corresponding Wilson loop which is in turn defined by a specific closed path on the lattice. The most apparent way to define a path on the lattice is to list the series of lattice sites it connects. For example, for a plaquette in the x-y plane, it can be

described by the following point series:

$$x_1 = (0,0,0,0) \qquad x_2 = (1,0,0,0)$$
$$x_3 = (1,1,0,0) \qquad x_4 = (0,1,0,0).$$

However, the point series fixes the plaquette at the origin of lattice while a sub-action should be summed over all possible positions. It is therefore more appropriate to define a lattice as a series of vectors:

$$x_{n+1} - x_n = s_n \hat{\mu}_i \qquad x_0 = x_l, \tag{3.30}$$

where l is the circumference of the Wilson loop and s_n of value $\pm 1$is used to describe the directions of the unit vectors. With x_0 unfixed, the series of vectors are well-suited to describe the sub-action. It also possesses a one-to-one correspondence to a link field formulation of a Wilson loop in the sense that we can write a general Wilson loop as

$$C = e^{igs_1 A_{\mu_1}} \cdots e^{igs_l A_{\mu_l}} \tag{3.31}$$

without losing any generality. Recall the explicit definition of $S(C)$:

$$\begin{aligned} S(C) &= TrRe(1-C) \\ &= -\frac{1}{2} Tr(e^{igs_1 A_{\mu_1}(x)} \cdots e^{igs_l A_{\mu_l}(x)} + e^{-igs_l A_{\mu_l}(x)} \cdots e^{-igs_1 A_{\mu_1}(x)} - 2), \end{aligned} \tag{3.32}$$

we want to reexpress the sub-action in terms of the summation of vertex functions of different numbers of gluons:

$$\begin{aligned} S(C) = \sum_{m=2}^{\infty} \frac{(ig)^m}{m!} \int \frac{d^4 p_1}{(2\pi)^4} \cdots \int \frac{d^4 p_m}{(2\pi)^4} (2\pi)^4 \delta(\sum_{i=1}^{n} p_i) \\ A_{\mu_1}^{a_1}(p_1) \cdots A_{\mu_m}^{a_m}(p_m) V_{a_1 \cdots a_m}^{\mu_1 \cdots \mu_m}(p_1 \cdots p_m), \end{aligned} \tag{3.33}$$

where repeated indices imply summations. Now the question of how to generate the vertex functions from a sub-action can be stated more explicitly as how to obtain the coefficient V of m gluon term given a Wilson loop C of particular shape and circumference l.

The first scenario can be described as follows. For the Wilson loop expression $e^{igs_1 A_{\mu_1}(x)} \cdots e^{igs_l A_{\mu_l}(x)}$, we can assume that the first gluon field $igs_{k_1} A_{\mu_{k_1}}$ comes from the link field $e^{igs_{k_1} A_{\mu_{k_1}}(x)}$ where $1 \leq k_1 \leq l$. Now, the second gluon field can be expressed as $igs_{k_2} A_{\mu_{k_2}}(x)$ only where $k_1 \leq k_2 \leq l$ so that the ordering is preserved. In this way we get m gluon fields:

$$(ig)^m (s_{k_1} A_{\mu_{k_1}}(x)) \cdots (s_{k_m} A_{\mu_{k_m}}(x)), \qquad 1 \leq k_1 \leq k_2 \cdots \leq k_m \leq l. \tag{3.34}$$

In order to obtain all m gluon contributions we need to sum over all possible series of $\{k_1, k_2 \cdots k_m\}$ weighted by proper factors:

$$\begin{aligned} &\sum_{1\le k_1\le k_2\cdots\le k_m} -\frac{(ig)^m}{2} f(\{k_1\cdots k_m\})\times \\ &Tr((s_{k_1}A_{\mu_{k_1}}(x))\cdots(s_{k_m}A_{\mu_{k_m}}(x)) + (-1)^m (s_{k_m}A_{\mu_{k_m}}(x))\cdots(s_{k_1}A_{\mu_{k_1}}(x)), \end{aligned} \tag{3.35}$$

where $f(\{k_1\cdots k_m\})$ is the factor related to a particular series of $k_i's$. The factor can be understood easily. We want to pick m gluon fields from l link fields with a fixed order. If we have α_i gluon fields coming from ith link field, the corresponding symmetry factors have to be removed since there is no order within such α_i fields. α_i can be defined as follows:

$$\alpha_i = \sum_{j=1}^{m} \delta_{i,k_j}, \qquad \text{where} \qquad 1 \le i \le l. \tag{3.36}$$

After removal of symmetry factors 3.35 becomes:

$$\begin{aligned} &-\sum_{1\le k_1\le k_2\cdots\le k_m} \frac{(ig)^m}{2}\frac{1}{\alpha_1!\alpha_2!\cdots\alpha_l!}\times \\ &Tr((s_{k_1}A_{\mu_{k_1}}(x))\cdots(s_{k_m}A_{\mu_{k_m}}(x)) + (-1)^m (s_{k_m}A_{\mu_{k_m}}(x))\cdots(s_{k_1}A_{\mu_{k_1}}(x)). \end{aligned} \tag{3.37}$$

We can rewrite the target form of $S(C)$ in 3.33 as follows:

$$S(C) = \sum_{m=2}^{\infty} \frac{1}{m!} S_m. \tag{3.38}$$

Combining this expression and 3.37, we can identify that:

$$\begin{aligned} S_m = &-(ig)^m \sum_x \sum_{1\le k_1\le k_2\cdots\le k_m} \frac{(ig)^m}{2}\frac{m!}{\alpha_1!\alpha_2!\cdots\alpha_l!}\times \\ &Tr((s_{k_1}A_{\mu_{k_1}}(x))\cdots(s_{k_m}A_{\mu_{k_m}}(x)) + (-1)^m (s_{k_m}A_{\mu_{k_m}}(x))\cdots(s_{k_1}A_{\mu_{k_1}}(x)). \end{aligned} \tag{3.39}$$

In order to express S_m in momentum space, we need to Fourier transform every gluon field:

$$A_{\mu_{k_i}}(x_{k_i}) = \int \frac{d^4p_i}{(2\pi)^4} e^{ip_i x + ip_i \tilde{x}_{k_i}/2} \delta_{\mu_i,\mu_{k_i}} T^{a_i} A^{a_i}_{\mu_i}(p_i). \tag{3.40}$$

In the above expression, we make use of the fact that the gauge field is defined at the middle point of the corresponding link. If we define $x \equiv x_1$ and $\tilde{x}_i \equiv x_i - x$, we will have

$\bar{x_i} = (\tilde{x_i} + \tilde{x_{i+1}})/2$. The Kronecker delta is present to ensure the correct polarization of gauge field. After transforming every gluon field in 3.39, we make use of the fact that:

$$\sum_x e^{i(p_1+p_2+\ldots+p_m)x} = (2\pi)^4\delta(p_1+p_2+\ldots+p_m). \tag{3.41}$$

After some algebra, we get:

$$\begin{aligned} S_m = &-(ig)^m \sum_{1\le k_1\le k_2\cdots\le k_m} \frac{(ig)^m}{2}\frac{m!}{\alpha_1!\alpha_2!\cdots\alpha_l!}\int\frac{d^4p_1}{(2\pi)^4}\cdots\int\frac{d^4p_m}{(2\pi)^4} \\ &\times(2\pi)^4\delta(p_1+p_2+\ldots+p_m)s_1{}^{\alpha_1}\ldots s_l{}^{\alpha_l}Tr(T^{a_1}\cdots T_{a_m}+(-1)^m T^{a_m}\cdots T_{a_1}) \\ &\times(\delta_{\mu_1,\mu_{k_1}}e^{ip_1\bar{x}_{k_1}/2}\ldots\delta_{\mu_m,\mu_{k_m}}e^{ip_m\bar{x}_{k_m}/2})A^{a_1}_{\mu_1}(p_1)\ldots A^{a^m}_{\mu_m}(p_m). \end{aligned} \tag{3.42}$$

We can define the trace of matrices as a color factor:

$$C_m^{a_1\ldots a_m} = Tr(T^{a_1}\cdots T_{a_m}+(-1)^m T^{a_m}\cdots T_{a_1}). \tag{3.43}$$

Then we denote other parts by a function:

$$\begin{aligned} Y^m_{\mu_1\ldots\mu_m}(p_1,\ldots,p_m) = &-\sum_{1\le k_1\le k_2\cdots\le k_m}\frac{1}{2}\frac{m!}{\alpha_1!\alpha_2!\cdots\alpha_l!} \\ &\times s_1{}^{\alpha_1}\ldots s_l{}^{\alpha_l}(\delta_{\mu_1,\mu_{k_1}}e^{ip_1\bar{x}_{k_1}/2}\ldots\delta_{\mu_m,\mu_{k_m}}e^{ip_m\bar{x}_{k_m}/2}). \end{aligned} \tag{3.44}$$

With these simplified notations, 3.42 becomes:

$$\begin{aligned} S_m = &(ig)^m\int\frac{d^4p_1}{(2\pi)^4}\cdots\int\frac{d^4p_m}{(2\pi)^4}(2\pi)^4\delta(p_1+p_2+\ldots+p_m) \\ &\times(A^{a_1}_{\mu_1}(p_1)\ldots A^{a^m}_{\mu_m}(p_m))C_m^{a_1\ldots a_m}Y^m_{\mu_1\ldots\mu_m}(p_1,\ldots,p_m). \end{aligned} \tag{3.45}$$

Given the target form of $S(C)$ in 3.33, we can identify the vertex function now. According to Bose-Einstein statistics the vertex function should be symmetric under permutation of any two gluons. Therefore we can obtain:

$$V^{a_1\cdots a_r}_{\mu_1\cdots\mu_r}(p_1,\ldots,p_m) = \frac{1}{m!}\sum_{\mathcal{P}_r}C_m^{a_1\ldots a_m}Y^m_{\mu_1\ldots\mu_m}(p_1,\ldots,p_m), \tag{3.46}$$

where $\mathcal{P}_r$ is a set containing all possible permutations of $\{1,\cdots,m\}$. One needs only to use a computer to generate the un-symmetrized expression of vertex function since the symmetrization can be implemented easily even by hand. It is noticeable that both the color

factor $C_m^{a_1\ldots a_m}$ and the function $Y^m_{\mu_1\ldots\mu_m}(p_1,\ldots,p_m)$ are determined by the complete set of possible $\{k_1,\ldots,k_m\}$. A dictionary can be set up indexed by $\{k_1,\ldots,k_m\}$ with the entries of $C_m^{a_1\ldots a_m}$ and $Y^m_{\mu_1\ldots\mu_m}(p_1,\ldots,p_m)$. One can refer to [21] for a explicit example.

Since the algorithm is very important, it will be instructive if we can understand 3.42 from a second scenario. We consider again a Wilson loop with circumference l:

$$U_1\ldots U_l = e^{igs_1A_{\mu_1}}\cdots e^{igs_lA_{\mu_l}},$$

where the link field and its hermitian conjugation are both denoted as U_i. Now let's define:

$$U(i,l)\equiv U_i\ldots U_l, \qquad \text{where} \qquad 1\le i\le l. \tag{3.47}$$

Now we can define the Wilson loop recursively:

$$\begin{aligned} &U(1,l)=U_1U(2,l),\\ &\quad\vdots \qquad\qquad \text{where} \qquad 1\le i\le l-1,\\ &U(i,l)=U_iU(i+1,l). \qquad\quad U(l,l)\equiv U_l. \end{aligned} \tag{3.48}$$

Let's start from the first chain of the recursion. We can expand U_1 without difficulty:

$$U_1 = 1+igs_1A_{\mu_1}(x)+\frac{1}{2!}(igs_1A_{\mu_1}(x))^2+\ldots=\sum_{n_1=0}^{\infty}\frac{1}{n_1!}(igs_1A_{\mu_1}(x))^{n_1}.$$

Now, in order for the vertex function to contain only m gluon fields, the number of gluon field contributed from U_1, denoted as α_1, should not be larger than m. It is also apparent that the number of gluon fields from $U(2,m)$ should compensate α_1 in such a way that the total number of gluon fields is m. We can now write explicitly for the first chain that:

$$\sum_{\alpha_1=0}^{l}\sum_{\alpha(2,l)=0}^{l}\frac{1}{\alpha_1!}(igs_1A_{\mu_1}(x))^{\alpha_1}f(2,l)(igs_1A_{\mu_1}(x))^{\alpha(2,l)}\delta(\alpha_1+\alpha(2,l)-m), \tag{3.49}$$

where $f(2,l)$ denotes the contribution to overall coefficient from $U(2,l)$. Now we need to decompose $U(2,l)$ into $U_2U(3,l)$. It proceeds in the same way as the first decomposition only this time our upper limit for the number of gluons becomes $\alpha(2,l)$ instead of the m. We can proceed recursively using $U(i,l)=U_iU(i+1,l)$ until $i=l-1$. The final expression we get for the m gluon contribution from $U(1,l)$ is:

$$\begin{aligned} &\sum_{\alpha_1=0}^{m}\sum_{\alpha_2=0}^{m}\cdots\sum_{\alpha_l=0}^{m}\frac{\delta(\sum_{i=1}^{l}\alpha_i-m)}{\alpha_1!\ldots\alpha_l!}\\ &\times(ig)^m(s_1^{\alpha_1}\ldots s_l^{\alpha_l})(A_{\mu_1}(x)^{\alpha_1}\ldots A_{\mu_l}(x)^{\alpha_l}). \end{aligned} \tag{3.50}$$

Recall the definition of $S(C)$ in 3.29, 3.32 and 3.38, it can be identified that:

$$\begin{aligned} S_m = &-\sum_x \sum_{\alpha_1=0}^{m} \sum_{\alpha_2=0}^{m} \cdots \sum_{\alpha_l=0}^{m} \frac{\delta(\sum_{i=1}^{l} \alpha_i - m)}{2\alpha_1! \ldots \alpha_l!} \\ &\times (ig)^m (s_1^{\alpha_1} \ldots s_l^{\alpha_l})(A_{\mu_1}^{a(1)} \cdots A_{\mu_1}^{a(\alpha_1)} \ldots A_{\mu_l}^{a(m-\alpha_l+1)} \cdots A_{\mu_l}^{a(m)}) \\ &\times Tr(T^{a(1)} \cdots T^{a(m)} + (-1)^m T^{a(m)} \cdots T^{a(1)}). \end{aligned} \tag{3.51}$$

Up to some trivial differences, 3.51 is essentially the same as 3.39. All the development for the momentum space representation can be carried over. It is evident $\alpha_1, \cdots, \alpha_l$ can determine the form of vertex as well from this perspective.

The two scenarios presented above are indistinguishable from each other in the current problem. However, the second scenario actually presents a more general understanding of Lüscher's algorithm. The action of interest S might be decomposed into a set of basic operators(not necessarily link fields) $\{O_1, O_2 \ldots O_n\}$. Vertex functions of S will be convolutions of vertex functions of $\{O_1, \ldots, O_n\}$. To make the statement more concrete, consider $n = 2$ and

$$\begin{aligned} O_1 &= \sum_{n=0}^{\infty} g^n K_{\mu_1 \ldots \mu_n}^{a_1 \ldots a_n}(n) A_{\mu_1}^{a_1} \cdots A_{\mu_n}^{a_n} \\ O_2 &= \sum_{n=0}^{\infty} g^n Q_{\mu_1 \ldots \mu_n}^{a_1 \ldots a_n}(n) A_{\mu_1}^{a_1} \cdots A_{\mu_n}^{a_n}, \end{aligned} \tag{3.52}$$

The order g^m vertex function of $S = O_1 O_2$ can be obtained by convoluting the two parts:

$$S_m = \sum_{n_1=0}^{m} \sum_{n_2=0}^{m} \delta(n_1 + n_2 - m) K_{\mu_1 \ldots \mu_{n_1}}^{a_1 \ldots a_{n_1}}(n_1) Q_{\mu_1 \ldots \mu_{n_2}}^{a_1 \ldots a_{n_2}}(n_2) A_{\mu_1}^{a_1} \cdots A_{\mu_m}^{a_n}. \tag{3.53}$$

The convolution can also be carried out in momentum space. In short, such an observation enhances our flexibility in vertex function generation and will be proven to be useful. One can refer to [43] and [45] for both momentum space convolution and the application of the idea.

3.2.2 Lüscher and Weisz's algorithm: fermionic action

After discussing the implementation of Lüscher's algorithm in gauge action, it is easy to generalize to the fermionic action. A fermionic lattice action is made up of Wilson lines

instead of Wilson loops. As was displayed in Eq. 2.10, a typical Wilson line can be written as:

$$\bar{\psi}(x)U_\mu(x)U_\nu(x+\hat{\mu})U_\mu(x+\hat{\mu}+\hat{\nu})\psi(x+2\hat{\mu}+\hat{\nu}). \tag{3.54}$$

We could employ either of the two scenarios discussed in Section 3.2.1 to generate an order-preserving vertex involving two fermions and m gluons.

There are several simple points worth mentioning. First of all, Fourier transformation of vertex functions should take into account the position shift in fermion fields. In the case of Eq. 3.54, there will be an extra $e^{i(2p_\mu+p_\nu)}$ in the momentum space form of the vertex functions. Secondly, since there is no requirement to take the real part or trace in the definition of fermionic action, the color factor now will be a product of matrices. For an m gluon interaction, it is:

$$C_m^{a_1\cdots a_m} = T^{a_1}\cdots T^{a_m}. \tag{3.55}$$

There will also be some changes of definition so that we can have open paths. They are all trivial to implement. One can refer to [21] for a more detailed description.

3.3 Twisted periodic boundary condition

Loop calculations in quantum field theories, no matter in the continuum or on the lattice, generally suffer from infrared divergences. While one can introduce gluon mass to reduce the infrared divergence to finite, this scheme is not gauge invariant by its nature. It is therefore preferable to have a consistent gauge invariant infrared cut-off. Twisted periodic boundary conditions provide us such a cut-off. Furthermore, it simplifies the color structure in the automatic vertex generation and also provides a spectrum which facilitates the on-shell improvement programme. All the points above constitute the importance of the technique and necessitate a detailed review of it.

3.3.1 Basic formulism: pure gauge action

The twisted periodic boundary condition was first introduced to continuum quantum field theory by 't Hooft[46]. Its lattice application was explored by many lattice theorists including Lüscher and Weisz[12]. Its basic idea is simple. While normal periodic boundary

conditions impose fields defined at one edge of lattice which have identical values as those defined at the other edge, or mathematically:

$$U_\mu(x+L\hat{\nu}) = U_\mu(x), \tag{3.56}$$

where L is the size of lattice along the ν direction, twisted periodic boundary conditions relaxes the requirement from identical to identical up to a constant gauge transformation:

$$U_\mu(x+L\hat{\nu}) = \Omega_\nu U_\mu(x)\Omega_\nu^\dagger. \tag{3.57}$$

Imposing the boundary condition along only one direction is trivial. It can be shown that the twisted periodic boundary condition is equivalent to periodic boundary condition if we redefine link fields as follows:

$$\tilde{U}_\nu(x) = \begin{cases} U_\nu(x) & \text{if } 0 < x_\nu < L \\ U_\nu(x)\Omega_\nu & \text{if } x_\nu = L \end{cases} \tag{3.58}$$

Thus a twist in one direction does not make any difference physically and is not interesting to us.

Twisted periodic boundary conditions in two directions(x,y for the current work) will however generate interesting consequences. First, let's write the link field $U_\mu(x)$ explicitly as $U_\mu(x,y,z,t)$ with x,y,z and t defined in the range of $(0,L)$ understood. After defining link fields on all points within the lattice, there are generally two ways of defining the link field at point $(x+L,y+L,z,t)$ since the two boundaries can be crossed in different orders:

$$\begin{aligned} U_\mu(x+L,y+L,z,t) =& \Omega_x U_\mu(x,y+L,z,t)\Omega_x^\dagger = \Omega_x\Omega_y U_\mu(x,y,z,t)\Omega_y^\dagger\Omega_x^\dagger, \\ U_\mu(x+L,y+L,z,t) =& \Omega_y U_\mu(x+L,y,z,t)\Omega_y^\dagger = \Omega_y\Omega_x U_\mu(x,y,z,t)\Omega_x^\dagger\Omega_y^\dagger, \end{aligned} \tag{3.59}$$

where in the first line the x boundary is crossed first while in the second line the y boundary is crossed first. These two ways must result in the same definition for consistency:

$$\Omega_x\Omega_y U_\mu(x,y,z,t)\Omega_y^\dagger\Omega_x^\dagger = \Omega_y\Omega_x U_\mu(x,y,z,t)\Omega_x^\dagger\Omega_y^\dagger. \tag{3.60}$$

After some trivial algebra, one can derive:

$$[\Omega_x^\dagger\Omega_y^\dagger\Omega_x\Omega_y, U_\mu(x,y,z,t)] = 0. \tag{3.61}$$

According to group theory,$\Omega_x^\dagger\Omega_y^\dagger\Omega_x\Omega_y$ must be a element of the central group of $SU(N)$, namely $Z(N)$, in order for 3.61 to hold for arbitrary link field U_μ. Elements of $Z(N)$ can be represented by $e^{2\pi ni/N}$ where $n = 1 \ldots N-1$. In the current work the following convention is adopted:

$$\begin{aligned} \Omega_x^\dagger\Omega_y^\dagger\Omega_x\Omega_y &= e^{2\pi i/N} \equiv z \\ \Omega_x\Omega_y &= z\Omega_y\Omega_x. \end{aligned} \tag{3.62}$$

It was shown in [12][2] that the phase z can't be eliminated by a simple field redefinition 3.58. Explicit forms of Ω's, although irrelevant to our purpose, are found in [48]. We need only know that:

$$\Omega_\nu^N = (-1)^{N-1}I. \tag{3.63}$$

In Lattice perturbation theory we expand link fields in terms of the gauge potential $A_\mu(x)$. It is apparent that gauge potential should satisfy the same boundary condition:

$$A_\mu(x+L\hat{\nu}) = \Omega_\nu A_\mu(x)\Omega_\nu^\dagger. \tag{3.64}$$

For reasons which will be evident later, we decompose $A_\mu(x)$ into Fourier modes as follows:

$$A_\mu(x) = \frac{1}{NL^4}\sum_p \Gamma_p e^{ipx+i\frac{p_\mu a}{2}} A_\mu(p). \tag{3.65}$$

Γ_p is a set of color matrices which are momentum dependent. One can find a convention for the explicit form of Γ_p in [21]:

$$\Gamma_p = \Omega_x^{-n_y}\Omega_y^{n_x}z^{-n_xn_y}. \tag{3.66}$$

There is an interesting and important mixing of color and momentum degrees of freedom. Γ_p have a set of useful properties[12]:

$$\begin{aligned} &\Gamma_p = \Gamma_{p'} && \text{if } p_x = p'_x \text{ and } p_y = p'_x. \\ &\Gamma_p = I && \text{if } p_x = p_y = 0 \\ &Tr\Gamma_p = 0 && \text{unless } p_x = p_y = 0 \\ &\Gamma_p^\dagger = Z(p)\Gamma_{-p}, \\ &\Gamma_p\Gamma_{p'} = Z(p,p')\Gamma_{p+p'}, \end{aligned} \tag{3.67}$$

[2] A pedagogical description can be found in [47].

where $Z(p)$ and $Z(p,p')$ are all phase factors which vary as different choices are made for the explicit form of Γ_p.

Application of 3.65 to both sides of 3.64 reveals:

$$\Omega_\nu \Gamma_p \Omega_\nu^\dagger = e^{ip_\nu L}\Gamma_p. \tag{3.68}$$

Let's apply the transformation $N-1$ times more on the righthand side of 3.68 and make use of 3.63:

$$\Gamma_p = e^{iNp_\nu L}\Gamma_p. \tag{3.69}$$

This can be solved by a different quantization from normal periodic boundary condition:

$$p_\nu = \frac{2\pi n_\nu}{NL}, \qquad n_\nu = 1,2,\ldots \tag{3.70}$$

The new quantization can be viewed from two perspectives. One can argue that it generates finer resolution in momentum space for a given box size while it can also be understood as a way to reduce finite volume effects since a "larger" box size is obtained. Indeed these applications of twisted periodic boundary conditions are discussed in the literature. However, for our purposes, the important point is that zero modes are eliminated; one need only notice that for $n_x = n_y = 0(\text{modulo } N)$ we have $\Gamma_p = I$. According to group theory $Tr(A_\mu(x))$ should be 0 so that the generators of $SU(N)$ will remain traceless. It can't be the case unless:

$$A(p_x = 0(\text{modulo } N), p_y = 0(\text{modulo } N), p_z, p_t) = 0. \tag{3.71}$$

Effectively we exclude the troublesome zero momentum mode from our theory gauge invariantly.

The process above can be understood from an analysis of the number of degrees of freedom. In the normal basis we have L^4 momentum degrees of freedom and N^2-1 color degrees of freedom. Combining them together the total number of total degrees of freedom become $(N^2-1)L^4$. In the twisted basis, there are L^2 degrees of freedom along untwisted directions. For the twisted directions, the number of degrees freedom seems to be N^2L^2 according to 3.70. However, properties of $SU(N)$ group eliminates L^2 degrees of freedom. In summary we have $(N^2-1)L^4$ degrees of freedom as well. Twisted periodic boundary conditions can be regarded as a way to align zero momentum degrees of freedom with a $U(1)$ degree of freedom in $U(N) = SU(N) \otimes U(1)$ which drops out. It provides us with a general perspective to eliminate un-wanted degrees of freedom.

Twisted periodic boundary conditions can also be applied to three directions. However, such cases are not relevant to our discussion here and interested readers are referred to [47] and the references therein.

3.3.2 Basic formalism: fermionic case

Twisted periodic boundary conditions must also affect quarks for the sake of consistency. In order to apply the bilinear form 3.57, a new gauge group, the smell group $SU(3)_S$ is introduced. In additional to color, quarks now possess a new quantum number: smell. The smell group has no dynamical implications and quarks have a three-fold degeneracy under smell group.

Now, a quark field is represented by a 3 by 3 matrix in the color-smell basis. The equation of motion will be changed accordingly. For example, the mass term will become the trace of the product of two fermion matrices properly normalized:

$$\frac{1}{N}Tr[\bar{\psi}_{sc}\psi_{sc}]. \tag{3.72}$$

Other operators involving quark fields transform similarly. The new representation can be written in the plane wave expansion as well:

$$\psi(x) = \frac{1}{N}\sum_p \Gamma_p \psi(p) e^{ipx}. \tag{3.73}$$

However, since the representation is not related to generators of a Lie group, modulo N zero momentum modes are not excluded from the theory. This doesn't cause any trouble since fermion masses in our cases will act as infrared cut-offs by themselves.

3.3.3 Twisted Lattice Perturbation Theory

As was discussed in previous sections, once twisted periodic boundary conditions are imposed, normal color matrices T^a will be replaced by momentum dependent Γ_p's. Naturally, the automatically generated Feynman rules for lattice actions will be slightly different as well.

Let's review the process to generate Feynman rules introduced in Section 3.2.1. The only part in Eq. 3.42 involving color matrices are the color factor C_m. The color factor in

the twisted basis should be:

$$C_m(p_1,p_2,\ldots,p_m) = \frac{1}{N}Tr[\Gamma_{p_1}\cdots\Gamma_{p_m} + (-1)^m\Gamma_{p_m}\cdots\Gamma_{p_1}]. \tag{3.74}$$

Let's recall the last property listed in 3.67 $\Gamma_p\Gamma_{p'} = Z(p,p')\Gamma_{p+p'}$ and use it recursively to simplify 3.74. The color factor defined in the twisted basis becomes:

$$C_m(p_1,p_2,\ldots,p_m) = \frac{1}{N}Z(p_1,\ldots,p_m)Tr[\Gamma_{p_1+p_2+\ldots+p_m}], \tag{3.75}$$

where $Z(p_1,\ldots,p_m)$ is a phase factor determined by all momenta. We know from the third property in 3.67 that in order for the trace to be non-zero momentum components of the summation along twisted directions must be 0. This effectively enforces momentum conservation along twisted directions. In the end, the color factor is just a number.

However, the explicit dependence of Z on these momenta has different conventions due to the different phase conventions that one may adopt for the twist matrices Γ_p. For example, in [12] $Z(p,q)$ was defined to be $z^{\frac{1}{2}(<p,q>-(p,q))}$ where:

$$\begin{aligned}(p,q) &= n_x m_x + n_y m_y + (n_x+n_y)(m_x+m_y)\\ <p,q> &= n_x m_y - n_y m_x.\end{aligned} \tag{3.76}$$

(n_x,n_y) are momentum components of p along twisted directions while (m_x,m_y) are the counterparts of q. In [21] a simpler convention for $Z(p,q)$ is adopted. One can derive the Z factor for m momenta recursively.

Chapter 4

On-shell improvement programme

As was discussed in Section 2.3.2, improvement of the lattice action is necessary given the current computational power we have. Since the current work is primarily an improvement of the lattice action, it is therefore appropriate to give some detailed discussion of the philosophy of on-shell improvement programme. The previous works on the quenched on-shell improvement of the gauge action will also be introduced and summarized, which will serve as a conceptual basis for my work here. For a general overview of the on-shell improvement programme, one is referred to Section 1.3.

4.1 Scaling violation of a lattice action

We have been talking about finite lattice spacing errors loosely in previous Chapters. The errors can be described as the discrepancies between lattice results of a calculation on a lattice with finite spacing, and the "true" continuum result (neglecting other systematic errors).

Now consider a generic lattice action in two versions: version I with dependence of a explicitly preserved and version II with a set to be 1. In order for a lattice theory to be physically relevant, the correlation length ξ of continuum *QCD* must be reproduced as the continuum limit is approached. ξ is a finite value. For version I, the continuum limit is defined as $a \to 0$ or $\xi/a \to \infty$. It is now clear if we set $a = 1$ as in version II, the correlation length of such a lattice theory will diverge as the continuum limit is taken. This simple observation suggests that a second order phase transition occurs as a lattice

action is taken to its continuum limit. It provides us with a different perspective on the relation between lattice theory and continuum theory. We expect that in the vicinity of the phase transition all proper lattice actions will fall into the same universality class, in the other word different lattice actions should give identical expectation values of any n-point functions in the continuum limit.

Since there is a second order phase transition, renormalization equations can also be introduced to give us a clearer idea. Let's consider lattice as a scheme to regularize continuum QCD. The lattice spacing a is introduced to all spectral quantities and n-point functions as a dynamical scale. We generally have:

$$G^n(g_0,a) = a^{-\gamma}\tilde{G}^n(g_0,a), \tag{4.1}$$

where $\tilde{G}$ is dimensionless. In ideal case, we can find a renormalized coupling $\tilde{g}_0(a)$ so that:

$$a\frac{dG^n(\tilde{g}_0(a),a)}{da} = 0. \tag{4.2}$$

In this case, the lattice theory possesses a perfect scaling property which ensures identical critical behavior in the vicinity of second order phase transition. However, for a general lattice theory the scaling is violated to the order of a^2:

$$a\frac{dG^n(\tilde{g}_0(a),a)}{da} = O(a^2). \tag{4.3}$$

A lot of effort has been devoted to improving the scaling properties of lattice theory. For example, the perfect action developed by P. Hasenfraz[19] is designed to satisfy perfect scaling. The work here follows a more modest approach to the problem. It was first shown by K. Symanzik[49] that $O(a^2)$ scaling violations in all n-point functions can be simultaneously improved by improving the action and a field redefinition in the context of non-linear σ-model. The improvement condition was modified by Lüscher and Weisz[14] so that the scaling property of only spectral quantities is improved, hence the name "on-shell improvement". They also performed quenched improvement for the Wilson gauge action to one loop order[12][22] and one-loop improvement of dimension-six operators in the gluon action is hereafter referred to as $O(\alpha_s a^2)$ improvement. The quenched one loop improvement was carried out for both the Lüscher-Weisz action and the square action[23] by Snippe[50]. Order $\alpha_s a$ improvement for the Wilson fermion action was performed by

Wohlert[51]. Lüscher-Weisz's improved action is adopted generally by lattice community as a one-loop improved action. However, the quenched nature of their calculation is in some sense incomplete. Recalling the motivation of the thesis in Section 1.3, it is therefore necessary to perform an unquenched implementation of on-shell improvement of gauge actions so that unknown systematics from an quenched approximation can be consistently understood, constrained and controlled. The rest of the chapter will summarize works by Lüshcer, Weisz and Snippe whose approach will be adopted and generalized to include dynamical fermions in the current work.

4.2 Particle spectrum of the Twisted world

The scaling properties of a lattice action can be improved by adding irrelevant operators to the original action. As was shown in [14] there are generally four free parameters c_0, c_1, c_2, c_3 to fix. Among them c_1, c_2 and c_3 are the coefficients of different dimension six operators. One can write the improved gauge action in the following general form:

$$\begin{aligned} S[U] =& \frac{2}{g^2} \sum_{i=0}^{3} c_i(g^2) \sum_{C \in C_i} L(C) \\ \equiv& \frac{2}{g^2} \sum_{i=0}^{3} c_i(g^2) S_i, \end{aligned} \tag{4.4}$$

where C is a Wilson loop of a particular direction and C_i is a set of Wilson loops of particular shape. Here C_0 consists of all plaquettes while C_1, C_2 and C_3 consist of Wilson loops of shape a, b and c in Fig. 2.2 respectively. In order for the lattice action to yield the correct normalization in the continuum limit, one can impose:

$$c_0 + 8c_1 + 8c_2 + 16c_3 = 1 \tag{4.5}$$

and thereby reduce number of free parameters to 3: c_1, c_2, c_3. One can prove an isospectral transformation property[14] of improved action if only on-shell quantities are to be improved. With the aid of the transformation it can be shown that c_3(or c_1) can be shifted to be 0 to all orders of perturbation theory without any effect on physical observables. Generally the convention $c_3 = 0$ is adopted for on-shell improvement programmes.

Now we need to fix the two genuine free parameters c_1, c_2 so that order a^2 scaling violations can be removed from all on-shell quantities. The strategy is relatively straightforward: we will first choose two on-shell quantities, calculate them to a certain order(one-loop order in the current work) and then adjust the two coefficients to cancel a^2 errors in them. If the perturbative approach is legitimate and the calculation is carried out correctly, we expect the new lattice action with the two parameter fixed will have no a^2 scaling violations in any on-shell quantities. One of the quantities can be chosen as the heavy quark potential at physical distances[22]. However, one-loop calculation can be very difficult if a second on-shell quantity is chosen in continuum QCD thanks to the complicated diagram structure and vertex function in Lattice Perturbation theory. Lüscher and Weisz suggested to carry out the improvement on a different space-time setting to simplify the calculation, namely the twisted world.

In order to build the twisted world, one starts with a Euclidean space-time QCD which can be easily obtained by proper Wick rotations of QCD in Minkowski space-time. Two directions(x and y) are compactified to a finite extent L with twisted periodic boundary conditions imposed while the other two directions remain infinite. As was discussed in Section 3.3, momentum modes whose x and y components are 0(mod 3) are excluded from the system. Effectively one finds a tower of particles of different "masses" in the uncompactified two dimensional space. For example, the particle with lowest mass $2\pi/(3L)$ is denoted as the A "meson" while the B meson has mass $2\sqrt{2}\pi/(3L)$, which is the second smallest mass. Let's define m as follows:

$$m = \frac{2\pi}{3L}. \tag{4.6}$$

It is clear that the A meson mass is m and that the B meson mass is $\sqrt{2}m$. In the interacting theory, most of the particles are unstable with the exception of A and B. In [12], it was shown that A and B mesons can be created by a Polyakov line and hence they are physical particles in the twisted world. They can appear as asymptotic states in contrast to gluons which are always confined inside hadrons and never appear as asymptotic states. Now we have a whole new set of on-shell quantities at our disposal. We can choose two of them to implement on-shell improvement.

4.3 Self-energy of the A meson

The simplest on-shell quantity is the self energy or "mass" of A meson. It can be defined as the pole of the two point correlation function. Let's consider the two point correlation function in twist world:

$$< A(k)A(k') >= \frac{\int DAA(k)A(k')\exp(-S_g)}{\int DA\exp(-S_g)}. \tag{4.7}$$

In order to get the twisted color factor straight, we need to look into S_g in some detail. S_g will be of the following form if we adopt the Feynman gauge:

$$\begin{aligned} S_g &= -\frac{1}{2}\int dx_0 dx_3 \int_{-L/2}^{L/2} dx_1 dx_2 \sum_{a,\mu,\nu} (\partial_\mu A^a_\nu(x))^2 \\ &= -\int dx_0 dx_3 \int_{-L/2}^{L/2} dx_1 dx_2 \sum_{\mu\nu} Tr[(\partial_\mu A_\nu(x))^2], \end{aligned} \tag{4.8}$$

where $A_\nu = \sum_a A^a_\mu T^a$ and we used $Tr(T^a T^b) = 1/2\delta^{ab}$. With twisted periodic boundary conditions imposed on directions 1 and 2, $A(x)$ can be Fourier transformed in terms of momentum dependent color matrices similar to Eqn. 3.65:

$$A_\mu(x) = \frac{1}{NL^2}\sum_{p_1,p_2}\int\frac{dp_0}{2\pi}\int\frac{dp_3}{2\pi}\Gamma_p e^{ipx}A_\mu(p).$$

We then need to make use of the completeness relation:

$$\begin{aligned} &\int dx_0 dx_3 \int_{-L/2}^{L/2} dx_1 dx_2 e^{i(p+k)x} \\ =&(2\pi)^2 L^2 \delta_{p_1+k_1,0}\delta_{p_2+k_2,0}\delta(p_0+k_0)\delta(p_3+k_3) \\ \equiv&\frac{1}{N}\delta^4(p+k) \end{aligned} \tag{4.9}$$

and integrate over one of the momenta, say p. After all the dust settles down, the action in momentum space reads:

$$S_g = -\frac{1}{NL^2}\sum_{p_1,p_2}\int\frac{dp_0}{2\pi}\int\frac{dp_3}{2\pi}p^2 A(p)A(-p)Z(p,-p), \tag{4.10}$$

where $Tr(\Gamma_p\Gamma_{-p}) = Z(p,-p)N$. Now the derivation of the two point function is a standard path integral exercise to do and the result is:

$$< A_\mu(k)A_\nu(k') >= \delta^4(k+k')\left(-\frac{1}{2Z(k,-k)}\right)D_{\mu\nu}(k), \tag{4.11}$$

where $D_{\mu\nu} \equiv \frac{\delta_{\mu\nu}}{k^2}$ in the Feynman gauge. If we adopt Lüscher's convention for $Z(k,-k)$ in Eqn. 3.76, the $1/Z(k,-k)$ factor become $z^{-1/2(k,k)}$.

The poles of two point function come from $D_{\mu\nu}$ part. Consider an A meson with polarization vector $\varepsilon_\mu = \delta_{\mu,2}$; we can define a renormalized the two point function by summing all one-particle irreducible Feynman diagrams, and for convenience, contracting all the spin indices:

$$\begin{aligned} d(k) =& \sum_{\mu\nu} \varepsilon_\mu \varepsilon_\nu < A_\mu(k) A_\nu(k') > \\ =& \delta^4(k+k') \left(-\frac{1}{2} z^{-\frac{1}{2}(k,k)} \right) \frac{Z(k)}{k_0^2 + E(k)^2} \\ \equiv& \delta^4(k+k') \frac{\tilde{Z}(k)}{k_0^2 + E(k)^2}, \end{aligned} \tag{4.12}$$

where we absorb all the color factors into $\tilde{Z}(k)$ in the last line. Field strength renormalization factor $Z(k)$ can be extracted easily:

$$Z^{-1}(k) = -\frac{1}{2z^{\frac{1}{2}(k,k)}} \frac{\partial}{\partial k_0^2} d^{-1}(k)|_{k_0^2 = -E(k)^2}. \tag{4.13}$$

The mass of the A meson and renormalization factor $Z(k)$ at tree level can be calculated by setting $k = (im_A, m, 0, 0)$. The results were given in [12]:

$$\begin{aligned} m_A^{(0)} =& m \left(1 - (c_1 - c_2 + \frac{1}{12}) m^2 + O(m^4)) \right) \\ Z_A^{(0)} =& 1 - 2 \left(c_1 - c_2 + \frac{1}{12} \right) m^2 + O(m^4). \end{aligned} \tag{4.14}$$

Notice that even at the tree level both mass of the A meson and the $Z(k)$ factor differ from their continuum counterparts by an amount proportional to m^2, which can be identified as an order a^2 scaling violations by dimensional analysis. In order for the on-shell quantity m_A to be free of a^2 corrections, we need the tree level c_1 and c_2 to satisfy:

$$c_1^{(0)} - c_2^{(0)} = -\frac{1}{12}. \tag{4.15}$$

It is observed that by adopting 4.15 the tree level field strength renormalization $Z(k)$ is automatically order a^2 improved as well. However, it is an accident. Since $Z(k)$ is not an

on-shell quantity, in general it will not be order a^2 improved by the on-shell improvement programme.

As our primary goal is to improve m_A to one loop order here, we need to consider the one-loop contribution to m_A. Let's first expand $d(k)$ explicitly to one-loop order:

$$\begin{aligned} d(k) =& \sum_{\mu\nu} \varepsilon_\mu \varepsilon_\nu < A_\mu(k) A_\nu(k') > \\ =& D_{22}^{(0)}(k) + g^2 D_{22}^{(0)}(k) \pi_{22}(k) D_{22}^{(0)}(k), \end{aligned} \tag{4.16}$$

where $\pi_{\mu\nu}(k)$ is the vacuum polarization and the reader is reminded that the A meson is taken to have polarization in the "2" direction. We then take the inverse of $d(k)$ and Taylor expand it to the first order in g^2:

$$d^{-1}(k) = d_0^{-1}(k) + g^2 d_1^{-1}(k) = \frac{1}{D_{22}^{(0)}(k)} - g^2 \pi_{22}(k). \tag{4.17}$$

It can be seen that:

$$d_1^{-1}(k) = -\pi_{22}(k). \tag{4.18}$$

Let's consider the renormalized self energy $E(k)$ and the field strength renormalization $Z(k)$ where it is understood $E((im_A, m, 0, 0)) = m_A$. They can be expanded to one loop order as follows:

$$\begin{aligned} E(k) =& E_0(k) + g^2 E_1(k) \\ Z(k) =& Z_0(k) + g^2 Z_1(k). \end{aligned} \tag{4.19}$$

We can now express the inverse of $d(k)$ in a different way:

$$\begin{aligned} d^{-1}(k) =& \frac{k_0^2 + E(k)^2}{\tilde{Z}(k)} \\ =& \frac{k_0^2 + E_0(k)^2}{\tilde{Z}(k)} + \frac{2g^2 E_0(k) E_1(k)}{\tilde{Z}_0(k)} \end{aligned} \tag{4.20}$$

Comparing it with 4.17 the expression for the self-energy at one-loop order is obtained:

$$E_1(k) = -\frac{\tilde{Z}_0(k)}{2E_0(k)} \pi_{22}(k) = \frac{Z(k)}{4z^{\frac{1}{2}(k,k)} E_0(k)} \pi_{22}(k). \tag{4.21}$$

We expect $E_1((im_A, m, 0, 0)) = m_A^{(1)}$. Similarly to $m_A^{(0)}$, $m_A^{(1)}$ can be expanded as follows:

$$m_A^{(1)} = m(a_0 + a_1 m^2 + O(m^4)). \tag{4.22}$$

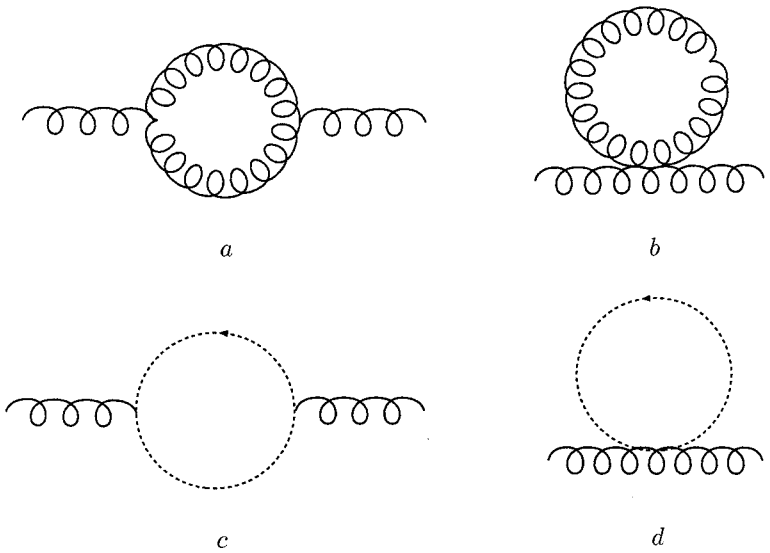

Figure 4.1: One loop contributions come from gluon and ghost loops in the quenched approximation.

It is up to the counter terms coming from $c_1^{(1)}, c_2^{(1)}$ to cancel out the order a^2 violation:

$$m_A^{(1)} = m(m_A^{(1)} - (c_1^{(1)} - c_2^{(1)})m^2 + O(m^4)). \tag{4.23}$$

Comparing the two expansions, we can get our first condition on the one loop coefficients $c_1^{(1)}, c_2^{(1)}$:

$$c_1^{(1)} - c_2^{(1)} = a_1 \tag{4.24}$$

We can calculate one-loop self energy $m_A^{(1)}$ at a range of different L's and extract a_1 by fitting the calculation results to 4.22. There are four Feynman diagrams contributing to the vacuum polarization in the quenched calculation. A sketch of the diagrams can be found in Fig. 4.1.

As we will see in Section 4.4, explicit expressions for one loop field strength renormalizations are needed to extract the order $\alpha_s a^2$ scaling violations in the 3-meson coupling. It is easy to derive the expression for the A meson. Expanding Eqn. 4.13 to one loop order on both sides and making use of 4.18, we obtain:

$$Z_1(k) = Z_0^2(k)\left(\frac{\partial}{\partial k_0^2}\pi_{22}(k) - 2E_0(k)E_1(k)(\frac{\partial}{\partial k_0^2})^2\pi_{22}(k)\right)|_{k_0^2=-E_0(k)^2}. \tag{4.25}$$

The field strength renormaliztion for the B meson will be derived in next section.

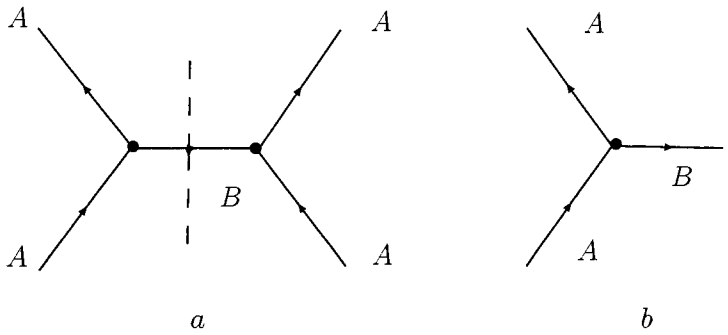

Figure 4.2: In the diagram *a* a possible channel of a A-A scattering is displayed. After the cut described by the dashed line, we get the tree level three point coupling in diagram *b*.

4.4 One-loop correction to the 3 meson coupling

The second on-shell quantity we choose is the three-meson coupling involving two A's and one B. Physically the coupling can be understood by analyzing A-A scattering. The scattering can happen through a point interaction as well as exchange of a B meson. As a result, it has a pole located at the mass of B meson. The residue of the pole can be interpreted as the square of a phenomenological three-meson coupling(Fig. 4.2). Through a closer look, one can conclude that the third components of both A mesons have to be imaginary in order for the B meson to be on-shell. Effectively we analytical continue the momentum components into the complex plane. The necessity of continuation can also be understood by a center of mass analysis: if the spatial momenta of both of the A's remain real, the center of mass energy is inevitably bigger than mass of the B so that the resulting B meson can not be on-shell.

The formal definition of the three point coupling is given in [22]:

$$i\lambda f(k,p,q) = \sqrt{Z_A(k)Z_A(p)Z_B(q)}\Gamma_3(k,p,q). \tag{4.26}$$

The momenta are chosen as follows:

$$\begin{aligned} k &= (iE_A(r), m, 0, ir), \qquad p = (-iE_A(r), 0, m, ir), \\ q &= (0, m, m, 2ir), \end{aligned} \tag{4.27}$$

where r can be adjusted so that B meson is on-shell. The tree level value of r is $\sqrt{2}m/2$.

$f(k,p,q)$ is the twisted color factor of the three point function:

$$f(k,p,q) \equiv \frac{1}{N} Tr\{\Gamma_k[\Gamma_p,\Gamma_q]\}. \tag{4.28}$$

$\Gamma_3(k,p,q)$ is the amplitude of three-meson scattering. Both field strength renormalizations of the A mesons are defined in the same way as Section 4.3. The field strength renormalization of the B meson can be derived similarly and its tree-level expansion is given in [50]:

$$Z_B(q) = 1 - (c_1 - c_2)m^2 + O(m^4). \tag{4.29}$$

The polarizations of the A's and B are defined as:

$$\begin{aligned} e(k) &= (0,0,1,0), \qquad e(p) = (0,1,0,0), \\ e(q) &= (0,1,-1,0). \end{aligned} \tag{4.30}$$

The tree level value of λ was derived explicitly in [50]:

$$\lambda = -8m\left(1 - \frac{1}{2}m^2[9(c_1 - c_2 + \frac{1}{12}) + 2c_2] + O(m^4)\right). \tag{4.31}$$

Following the same argument as in Section 4.3, the following condition must be satisfied in order for λ to be free of $O(a^2)$ scaling violations:

$$9(c_1^{(0)} - c_2^{(0)} + \frac{1}{12}) + 2c_2^{(0)} = 0. \tag{4.32}$$

Combining 4.32 with 4.15, we can obtain the values of $c_1^{(0)}$ and $c_2^{(0)}$ for the cancelation of $O(a^2)$ scaling violations in all on-shell quantities:

$$c_1^{(0)} = -\frac{1}{12}, \qquad c_2^{(0)} = 0. \tag{4.33}$$

We now need to calculate the $O(\alpha_s a^2)$ scaling violations by studying all the one-loop contributions to the three meson scattering. By adopting the quenched approximation, loop contributions from dynamical fermions are absent. The one-loop diagrams containing gluon and ghost internal loops are given in Fig. 4.3 and Fig. 4.4 respectively. Considering Eqn. 4.26, the left hand side can be expanded to one loop order as follows:

$$i\lambda f(k,p,q) = i\lambda_0 f(k,p,q) + ig^2\lambda_1 f(k,p,q) \tag{4.34}$$

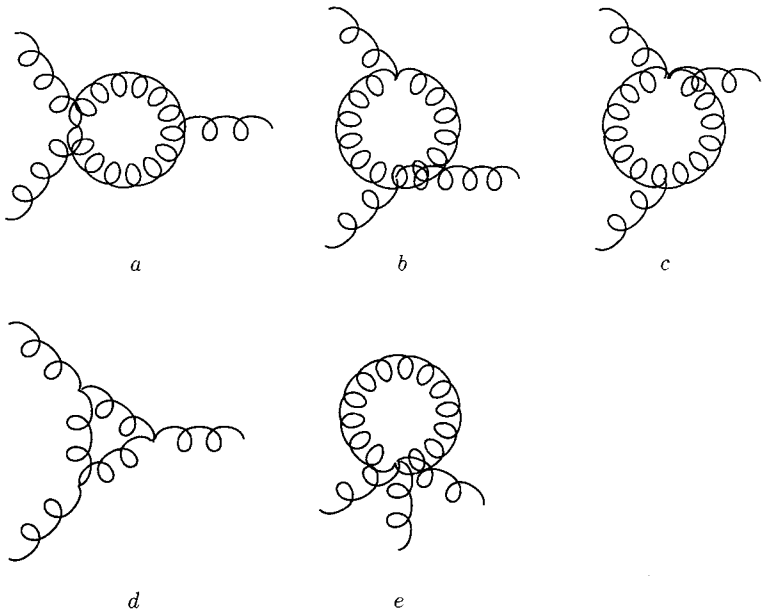

Figure 4.3: One loop diagrams containing a gluon loop.

The right hand side can also be expanded to one loop order. After a proper comparison λ_1 can be identified as follows:

$$i\lambda_1 f(k,p,q) = \sqrt{Z_A^{(0)}(k)Z_A^{(0)}(p)Z_B^{(0)}(q)}\left(\frac{1}{2}\Gamma_3^{(0)}\left(\frac{Z_A^{(1)}(k)}{Z_A^{(0)}(k)} + \frac{Z_A^{(1)}(p)}{Z_A^{(0)}(p)} + \frac{Z_B^{(0)}(q)}{Z_B^{(0)}(q)}\right) + \Gamma_3^{(1)}\right), \tag{4.35}$$

where $\Gamma_3^{(1)}$ encompasses all the one-loop diagram contributions to the three point coupling. In order to resolve the $O(\alpha_s a^2)$ scaling violations, we need to start with an $O(a^2)$ improved action. After applying 4.33 to 4.15,4.32,4.29 and 4.31 and plugging the results into 4.35, we obtain the expression for λ_1[50]:

$$\frac{\lambda_1}{m} = (1 - \frac{1}{24}m^2)\frac{\Gamma_3^{(1)}}{m} - 8\frac{d}{dk_0^2}\pi_{22}(k)\,|_{k_0^2=-E(k)^2} - 2(1-\frac{1}{12}m^2)\frac{d}{dq_0^2}\left(\frac{1}{2}\sum_{i,j} e(q)_i e(q)_j \pi_{ij}(q)\right)|_{q_0^2=0}. \tag{4.36}$$

We can then proceed the same way as in Section 4.3. Taking only contributions from one

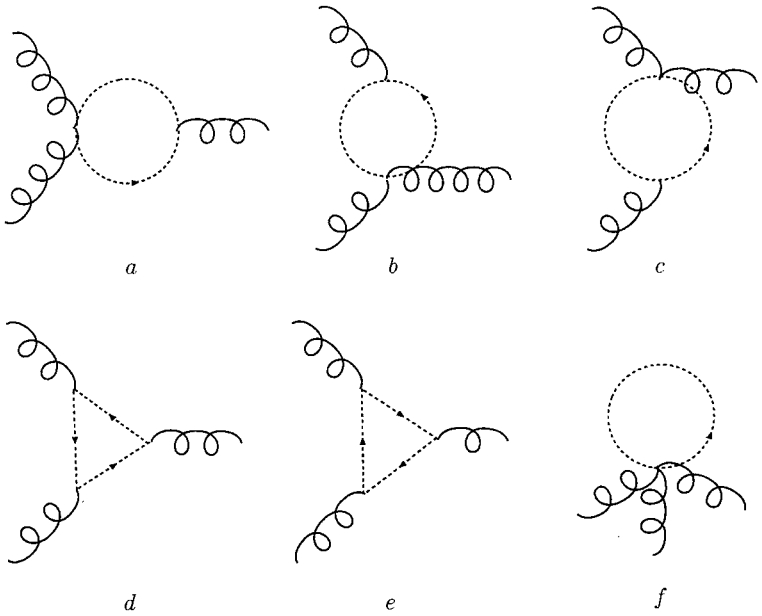

Figure 4.4: One loop diagrams containing a ghost loop.

loop diagrams into account, the explicit small m expansion of λ_1 was given in [12]:

$$\frac{\lambda_1}{m} = a_0 + b_0 \ln m + a_1 m^2 + a_2 m^4 + b_2 m^4 \ln m + O(m^6). \tag{4.37}$$

The counter term is of the following form:

$$\lambda^{(1)}/m|_{\text{counterterm}} = 4m^2 \left(9(c_1^{(1)} - c_2^{(1)}) + 2c_2^{(1)}\right). \tag{4.38}$$

In order for λ_1/m to be free of $O(a^2)$ scaling violations, the following condition must be satisfied:

$$4\left(9(c_1^{(1)} - c_2^{(1)}) + 2c_2^{(1)}\right) = -a_1. \tag{4.39}$$

Combining 4.39 with 4.24 we are able to determine $c_1^{(1)}$ and $c_2^{(1)}$.

Similar to the case of the self energy of A meson, different contributions from gluon loops, ghost loops and fermion loops are linearly summed to give the total one-loop amplitude. Given contributions from gluon loops and ghost loops are well established,by the work of Lüscher and Wesiz[12] as well as Snippe[50], the new calculation in this thesis is to explicitly compute the contributions of dynamical fermion loops to one-loop coefficients $c_1^{(1)}$ and $c_2^{(1)}$ and then add the contributions to the previous results of Lüscher and Weisz's or Snippe's to obtain complete results.

4.5 Facilities for numerical integration

The intrinsic complexity of lattice perturbation theory makes any analytical attempt to perform the loop integral infeasible. We need to use numerical integration programs to calculate one loop contributions. However, most numerical integration algorithms become very expensive if we want to resolve m^2 contribution when m is small. It is to Lüscher and Weisz's credit[12] again for inventing a finite sum approximation which allows accurate determination of loop integrals with errors understood through modest computational cost. The algorithm is quite simple to understand and essential to the current calculation. It will be described here in detail.

First of all, in the lattice world all momenta become sinusoidal functions which are periodic functions. Let's consider integration over a 1-dimensional periodic function $f(k)$ whose period is 2π:

$$F = \int_{-\pi}^{\pi} \frac{dk}{2\pi} f(k). \tag{4.40}$$

The integration can be approximated by finite a sum $I(T)$:

$$I(T) = \frac{1}{T} \sum_{v=1}^{T} f\left(\frac{2\pi}{T} v\right), \qquad T = 1,2\ldots \tag{4.41}$$

Physically we impose finite box size T on the given direction and impose periodic boundary conditions. The difference between the two is a finite volume effect. As was discussed in Section 2.7, such an effect generally falls exponentially as T increases. In the present case, we can prove it rigorously.

We can rewrite $I(T)$ as the special value of a function $g(t)$:

$$I(T) = \frac{1}{T} g(t) \mid_{t=0} = \frac{1}{T} \sum_{v=1}^{T} f\left(t + \frac{2\pi}{T} v\right) \mid_{t=0} . \tag{4.42}$$

It is clear that $I(t;T)$ is a periodic function whose period is $2\pi/T$. We can write $I(T)$ in terms of Fourier sum now:

$$I(T) = I(t;T) \mid_{t=0} = \frac{1}{T} \sum_{n=-\infty}^{\infty} c_n e^{-int} \mid_{t=0} = \frac{1}{T} \sum_{n=-\infty}^{\infty} c_n, \tag{4.43}$$

where the explicit form of c_n can be derived as follows:

$$\begin{aligned} c_n =& \frac{T}{2\pi}\int_{-\pi/T}^{\pi/T} dk g(k) e^{inTk} = T\int_{-\pi/T}^{\pi/T}\frac{dk}{2\pi}\sum_{v=1}^{T} f\left(k+\frac{2\pi}{T}v\right)e^{inTk} \\ =& T\sum_{v=1}^{T}\int_{(2v-1)\pi/T}^{(2v+1)\pi/T}\frac{d\tilde{k}}{2\pi}f(\tilde{k})e^{inT\tilde{k}} = T\int_{\pi/T}^{(2T+1)\pi/T}\frac{d\tilde{k}}{2\pi}f(\tilde{k})e^{inT\tilde{k}}, \end{aligned} \tag{4.44}$$

where we used variable transformation $\tilde{k} = k + 2\pi v/T$. After a trivial integration domain shift, we get:

$$c_n = T\int_{-\pi}^{\pi}\frac{dk}{2\pi}f(k)e^{ink}. \tag{4.45}$$

We can now return to 4.43 and obtain:

$$I(T) = \int_{-\pi}^{\pi}\frac{dk}{2\pi}f(k) + \sum_{n=1}^{\infty}\int_{-\pi}^{\pi}\frac{dk}{2\pi}f(k)(e^{ink}+e^{-ink}). \tag{4.46}$$

The first term of the right hand side is the integral we want to calculate. The difference between the finite sum and the integral is well represented by a series of Fourier integrals.

Let's consider the case that $f(k)$ has a pole whose distance from real k axis is ε. The series of Fourier integrals can now be performed one by one by contour integration. Clearly as a whole the difference will fall like $e^{-\varepsilon T}$ which confirms our intuition from before. The more rigorous understanding does have its advantage in the sense that it is clear that the convergence of the approximation will be greatly facilitated if we can push the pole away from the real axis while keeping the periodicity intact by a proper variable transformation. The transformation was also given by Lüscher[12]:

$$k = k' - \alpha\sin(k') \qquad \text{where} \qquad 0 \le \alpha < 1. \tag{4.47}$$

With the variable transformation the integration becomes:

$$F = \int_{-\pi}^{\pi}\frac{dk'}{2\pi}(1-\alpha\cos(k'))f(k(k')) = \int_{-\pi}^{\pi}\frac{dk'}{2\pi}\tilde{f}(k'). \tag{4.48}$$

The periodicity is preserved explicitly. The corresponding pole of $\tilde{f}(k')$ is denoted as $i\varepsilon'$ and it satisfies:

$$\varepsilon' - \alpha\sinh(\varepsilon') = \varepsilon. \tag{4.49}$$

In the limit of small ε' one can get an approximate relation:

$$\varepsilon' = \frac{\varepsilon}{1-\alpha}. \tag{4.50}$$

Table 4.1: One loop coefficients from quenched calculations.

Coefficients	Lüsher and Weisz[22]		Snippe[50]	
	$SU(2)$	$SU(3)$	$SU(2)$	$SU(3)$
$c_0^{(1)}$	0.1352	0.2370	0.135160(13)	0.23709(6)
$c_1^{(1)}$	−0.01396	−0.02521	−0.0139519(8)	−0.025218(4)
$c_2^{(1)}$	−0.00295	−0.00441	−0.0029431(8)	−0.004418(4)

It appears that the pole can be pushed away from real axis by a significant amount given α small enough.

4.6 List of previous results

The quenched calculation of $O(\alpha_s a^2)$ improvement for the Lüscher-Weisz action have been given in [22] and [50]. Their results agree with each other nicely and are summarized as in Table 4.1.

Chapter 5

Unquenched on-shell improvement of the gauge action

$O(\alpha_s a^2)$ on-shell improvement for a pure gauge action was discussed in the previous chapter under quenched approximation. As remarked in Section 1.3, quark loop contributions to the improvement coefficients are needed to explain the large scaling violation in the static quark potential calculation. These contributions will be calculated in the current chapter. It is understood that the coefficients $c_1^{(1)}$ and $c_2^{(1)}$ in this chapter are used to describe the quark loop contributions for the sake of simplicity. We adopt the order a^2 improved Asqtad action as our quark action:

$$L_q = \eta_\mu(x)\bar{\chi}(x)\left(\Delta'_\mu - \frac{a^2}{6}\Delta_\mu^3\right)\chi(x) + m\bar{\chi}(x)\chi(x), \tag{5.1}$$

where $\Delta_\mu(x)$ is the covariant derivative while $\Delta'_\mu(x)$ is also the covariant derivative with smeared links instead of ordinary link variables. Interested readers can refer to [52] for details of the action.

5.1 Fermions in the Twisted Tube

In order to calculate the contribution from dynamical fermions, we need first to put fermions in the twisted tube properly. The general approach to put fermions on a lattice with the twisted periodic boundary conditions was discussed in Section 3.3.2. As was discussed, the

major difference between fermions and bosons in the twisted tube is that the zero momentum modes(mode N) of fermions are not excluded. As a result, if we consider a massless fermion action for the twisted tube, both the A meson and the B meson would be unstable with regarding to decay into two fermions. The problem also manifests itself in the fact that the self-energy renormalization of the A meson will be infrared divergent. In order to keep mesons stable as well as prevent the infrared divergence, a infrared regulator should be introduced. One can adopt twisted anti-periodic boundary conditions:

$$\psi(x+L\hat{\mu}) = \Omega_\mu \psi(x) \Omega_\mu^\dagger e^{\frac{\pi}{N}}. \tag{5.2}$$

Following a similar argument to Section 3.3.2, it is observed that $\psi(x+NL\hat{\mu}) = -\psi(x)$. By Fourier transforming both sides, the possible momentum modes can be determined:

$$p_\mu = \frac{(2n+1)\pi}{NL}, \qquad \text{where} \qquad n = 0, \pm 1, \pm 2 \ldots \tag{5.3}$$

Effectively a mass gap of π/NL is produced. This method was used by Wohlert[51] to improve the Wilson fermion action to order $\alpha_s a$. However, the mass of the A meson is $2\pi/NL$ which is twice the mass gap while the mass of the B meson is larger than twice of the mass gap. The mesons are still unstable with regard to decay into two fermions. A fermion mass of large enough size will be adequate to solve the problem. Also, since we are introducing a fermion mass, we actually do not have to impose twisted boundary conditions, if we consider only the leading fermionic corrections to the gluon self-energy and three-point coupling. In fact, one can choose any boundary condition one likes to do the calculation as long as a sufficiently large quark mass m_q is present. Nonetheless, we have used twisted periodic boundary conditions, since these also allowed us to conduct some tests of our computations on the gluonic corrections that were previously analyzed by Lüscher and Weisz[12] as well as Snippe[50].

The importance of an appropriate infrared regulator can be understood more clearly from a loop-integration point of view. Let's consider one of the one loop diagrams shown in Fig 5.1. Consider the loop integral in Minkowski space-time, the integral should look like the following:

$$\int \frac{d^4k}{(2\pi)^4} \frac{f(q)}{\left((q-\frac{k}{2})^2 - m_q^2 + i\varepsilon\right)\left((q+\frac{k}{2})^2 - m_q^2 + i\varepsilon\right)}, \tag{5.4}$$

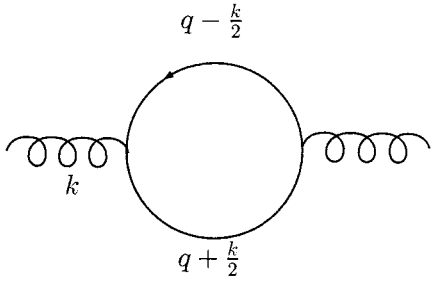

Figure 5.1: One of the fermionic one-loop contributions to A meson self energy

where $f(q)$ is an analytic function of q. The poles of q_0 can be solved as follows:

$$\begin{aligned} q_0 &= \frac{m}{2} \pm \sqrt{E_1^2 - i\varepsilon}, \\ q_0 &= -\frac{m}{2} \pm \sqrt{E_2^2 - i\varepsilon}. \end{aligned} \qquad \text{where} \qquad \begin{aligned} E_1^2 &= (\vec{q} - \frac{\vec{k}}{2})^2 + m_q^2 \\ E_2^2 &= (\vec{q} + \frac{\vec{k}}{2})^2 + m_q^2 \end{aligned} \tag{5.5}$$

It is clear that E_1 and E_2 share a minimum, m_q, although they can not reach their minima simultaneously. Let's bring both E_1 and E_2 to their minima together by considering zero three momenta $q = 0$ and $k = 0$: $E_1 = m_q$ and $E_2 = m_q$. Now the poles in the complex q_0 plane become:

$$\begin{aligned} q_0 &= \frac{m}{2} \pm (m_q - i\varepsilon) \\ q_0 &= -\frac{m}{2} \pm (m_q - i\varepsilon). \end{aligned} \tag{5.6}$$

It can be seen that unless $m_q > m/2$ there is no way to Wick rotating the integration contour to get a valid Euclidean theory in the infinite volume limit[1]. Therefore practically speaking one needs to keep the A meson stable. One can refer to Fig 5.2 for a visualized understanding.

5.2 General discussion of small m expansion

The necessity of introducing a gluon momentum(such as the mass gap m in the twisted world) as a tool to resolve discretization errors can be understood from a simple dimensional

[1] As for the twisted world, m can be made arbitrarily small as the size of twisted directions increases. It is therefore possible to perform Wick rotation for any quark mass bigger than zero.

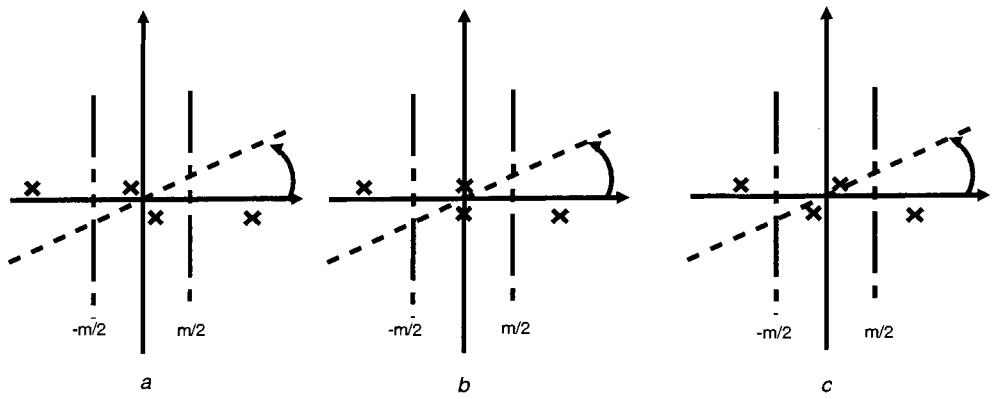

Figure 5.2: Diagrams a, b and c describe possible pole structures of 5.1 for $m_q > m/2$, $m_q = m/2$ and $m_q < m/2$ respectively under the assumptions that three momenta are 0 for both internal quarks. Poles of different colors come from different propagator. It is clear that Wick rotation can be performed without pole crossing in a. In the latter two diagrams Wick rotation can not be performed.

analysis point of view. In the quenched calculation, a is the only dimensionful scale in the problem unless a mass gap m is introduced by the twisted periodic boundary conditions. am is the only dimensionless variable in quenched calculations and therefore it's relatively easy to expand dimensionless quantities such as $m^{(1)}/m$ and $\lambda^{(1)}/m$ as polynomials of am.

After the introduction of dynamical fermions we are facing a more complicated question. While the quantities needed to be expanded are still dimensionless, we introduced another scale m_q into our problem. Now, there are two independent dimensionless variables: am and am_q. We have to examine the expansion problem more carefully before specific steps are decided to carry out the calculation.

First of all, we have three scales in the problem, namely a, m and m_q. As different limits are taken for them respectively, we will obtain different physical theories. $a \to 0$ corresponds to the continuum limit, we expect the continuum limit is well defined for both 4-dimensional Euclidean space and the $2+2$ twisted world. $m \to 0$ is the same as $L \to \infty$ for the twisted directions. By taking such limits, theories in the twisted world should become their counterparts in the 4-dimensional Euclidean space, which are well defined in the case of QCD. $m_q \to 0$ gives rise to theories containing massless fermions. While these theories' existence in both 4-dimensional Euclidean space and twisted world is beyond doubt, the

on-shell processes we are using now will lose their virtues for massless fermion theories in the twisted world. In summary, we expect the results of a calculation at particular am_q to yield good limits when m is taken to zero; we also expect calculations should have good continuum limits as $a \to 0$.

Bearing these observations in mind, let's consider a dimensionless function $f(am_q, am)$ which stands for either one-loop amplitude we are considering. We can Taylor-expand the function at fixed am_q around $am = 0$:

$$f(am_q, am) = g_0(am_q) + g_2(am_q)(am)^2 + g_4(am_q)(am)^4 + O((am)^6). \tag{5.7}$$

Now, the constant and coefficients are all functions of am_q. Their expansions will depend on various physical constrains. First consider $g_0(am_q)$. First of all, since we expect a well-defined continuum limit, there can not be negative powers of am_q in its expansion. However, there can generally be a logarithm term. In fact, π/a is the ultraviolet cut-off while m_q serves as the infrared cut-off in loop integrals. Generally there should be a logarithm divergence in the form of $\ln(am_q)$ even in the continuum. Positive powers of am_q are also expected. Summarizing these points, the expansion of $g_0(am_q)$ reads:

$$g_0(am_q) = d_{0,0}\ln(am_q) + g_{0,0} + g_{0,2}(am_q)^2 + O((am_q)^4). \tag{5.8}$$

Now let's focus our attention on $g_2(am_q)$. While all the discussions for $g_0(am_q)$ can be carried over, we can now include negative powers of am_q: $g_{2,-2}/(am_q)^2$. Combining these term with $(am)^2$ we have a continuum like contribution $g_{2,-2}m^2/m_q^2$. At fixed m^2 this term behaves like an infrared power divergence. As one can easily see we will in general have such continuum like contributions from $(am)^{2n}(n > 0)$ terms which signal an infrared power divergence of order $2n$. Since we need to match our lattice theory with continuum theory, these terms can be either preserved or excluded by examining the infrared properties of corresponding continuum one-loop amplitudes. For the sake of generality we preserve the term in our expansion here:

$$\begin{aligned} g_2(am_q) =& \frac{g_{2,-2}}{(am_q)^2} + \left(d_2 + \frac{d_{2,-2}}{(am_q)^2}\right)\ln(am_q) + g_{2,0} + (g_{2,2} + h_{2,2}ln(am_q))(am_q)^2 \\ &+ O((am_q)^4). \end{aligned} \tag{5.9}$$

Our next target will be $g_4(am_q)$. The new problem that it poses to us is the nature of the term $g_{4,-2}/(am_q)^2$. Combining with $(am_q)^4$ we get $g_{4,-2}m^2/m_q^2(am)^2$ which behaves

like an $O(a^2)$ discretization error. If we improve our action to the order $\alpha_s a^2$, we expect the a^2 expansion here will be identical to its counterpart in the continuum, which is 0. In other words, we expect elimination of all the terms like $g_{2n,-2(n-1)}m^{2(n-1)}/m_q^{2(n-1)}(am)^2$ once we finish our improvement. We can generalize the statement even further: once order $\alpha_s(am)^{2(n-s)}$ improvement is implemented, $g_{2n,-2(n-s)}m^{2s}/m_q^{2s}(am)^{2(n-s)}$ term will be eliminated from one-loop amplitudes. Given these arguments, since we are now implementing $\alpha_s(am)^2$ improvement, expansion of $g_4(am_q)$ reads:

$$\begin{aligned} g_4(am_q) =& \frac{g_{4,-4}}{(am_q)^4} + \frac{g_{4,-2}}{(am_q)^2} + g_{4,0} + (d_4 + \frac{d_{4,-4}}{(am_q)^4} + \frac{d_{4,-2}}{(am_q)^2})\ln(am_q) \\ &+ (g_{4,2} + h_{4,2}ln(am_q))(am_q)^2 + O((am_q)^4). \end{aligned} \tag{5.10}$$

The expansion process above suggests a possible way to carry out the calculation. For a particular one-loop quantity, say renormalization of the A meson self energy, one can first perform the calculation at fixed am_q for different lattice sizes L(and hence different m). By fitting the data set to the form 5.7, we can obtain $g_2(am_q)$. After repeating the process for different am_q's and then fitting the result to the form 5.9, we can obtain the constants and coefficients to a certain order, which enables us to improve the gauge action given any am_q. An important thing to note in the calculation is that the order of limits, first $am \to 0$ then $am_q \to 0$, can be preserved in current method. The process is more complicated simply because of the introduction of a third scale.

Let me summarize the expansion process I have just described. A general dimensionless function $f(am, am_q)$ was introduced. The expansion of the function $f(am, am_q)$ was performed under the physical constraints that the theory yields good limits as $a \to 0$ and that the theory is regular around $m = 0$ at fixed am_q. We have seen that lattice artifacts of different order and continuum terms are actually mixed together thanks to the possible negative powers of am_q.

A different parametrization where am and m/m_q are independent variables can be obtained by a simple resummation of different terms. This parametrization also implies a different fitting process. However, I am not going to discuss it in detail since the fitting process is not adopted in the current work.

5.3 Evaluation of systematic errors

One of the problems we face is to assess the systematic errors for each $g_2(am_q)$, from which we can obtain the systematic uncertainty of the improvement coefficients. Normally it's quite an easy question. One can fit the data for fixed am_q to Eqn 5.9 including some higher order terms, find their coefficients and assess systematic errors by calculating the higher order contributions. However, the simple approach turned to be troublesome in our case.

Our calculation results are of very high precision with relative errors as small as $10^{-8} - 10^{-9}$. We are forced to include a lot of higher order terms in order to make use of the full range of significant digits. To make the situation even worse, terms like $m^{2n}/m_q^{2n}(am)^{2l}$ can not be fully eliminated in higher order terms. It suggests some terms are suppressed only by orders of $(m/m_q)^2$ which is relatively large compared to am especially when am_q is small. As a result, higher order terms up to $g_8(am_q)(am)^8$ have to be included in the fit, some of the terms are only different by 1 order of magnitude, which makes the extraction of their coefficients very difficult. We also have no qualitative argument for the sizes of these coefficients to make a constrained fit applicable and reasonable. At this point, it is worthwhile to note that, in practice, an estimate of the $O(\alpha_s)$ coefficients in the gluon action of a few percent precision is more than adequate, since the uncalculated two-loop corrections are of order $10-20\%$ of the one-loop improvement. Hence for our purposes we can be content with fairly loose estimates of the systematic errors in our fits for expansions such as 5.7. It is evident from Fig.. 5.4, for example, that terms beyond the leading $O(am)^2$ discretization errors are very small (though a χ^2 fit requires such terms, given the high-degree of precision of our data).

For our purposes, we make a crude estimate of the systematic error in the fit to 5.7 by first estimating the coefficients using the full data set, and then using only one-half of the data set (at the smallest values of m), taking the difference in the two sets of fit results to estimate the systematic error.

Once we estimate the systematic uncertainties for every $g_2(am_q)$, we fit the upper-bound and lower-bound of $g_2(am_q)$ to Eqn 5.9 as well so that we get the uncertainties of all the relevant coefficients. However, since we are working at relatively large am_q's, the systematic error coming from the higher order terms in expansion 5.9 overshadows the systematic

error resulting from the errors of each $g_2(am_q)$. The observation serves as a further validation of our sloppy estimation of systematic errors of each $g_2(am_q)$: practically they are not the primary error source we need to be concerned with.

Last I want to point out that accurate estimation of systematics is possible only if we are working at small am_q and am's which are much smaller compared to the given am_q. Such an approach will be very expensive numerically. Since we are working at one-loop level, errors of a few percents will be enough for our results to be relevant phenomenologically and can be archived by our current setting. In one word, our calculation is practically adequate albeit not as rigorous as those by Lücsher and Weisz.

5.4 Renormalization of the A meson self-energy

We first calculate the renormalization of the A meson self energy. The analytical derivation follows the same route as Section 4.3 and bears the same final form 4.21

$$E_1(k) = \frac{Z(k)}{4z^{\frac{1}{2}(k,k)}E_0(k)}\pi_{22}(k).$$

The core of the expression is the vacuum polarization contracted with the A meson's polarization vector. Now we consider the fermion loop contribution as in Fig. 5.3. Following the first approach proposed in Section 5.2, we need to fix am_q first and calculate E_1 for different m's. After that, we then fit the data to the proposed form 5.7 to obtain $g_2(am_q)$. However, there are still some unsettled issues in the general expansion. We don't know whether there is a logarithmic divergence in $g_0(am_q)$ or whether there is a power divergence behaving like m^2/m_q^2. Although we can find these out through data fitting, it's better to have some physical arguments first.

As was remarked in the previous section, $g_0(am_q)$ will survive if we take the $m \to 0$ limit which transforms the theories in the twist tube to their counterparts on 4-dimensional Euclidean lattice. Furthermore, if we consider the $a \to 0$ limit for $g_0(am_q)$, it ought to have the same infrared behavior as the 4-dimensional continuum theory. In the continuum, only diagram a in Fig. 5.3 contributes. One need only to note that the contribution from the loop is transverse by itself:

$$\pi_{\mu\nu} = (k^2 g_{\mu\nu} - k_\mu k_\nu)\pi. \tag{5.11}$$

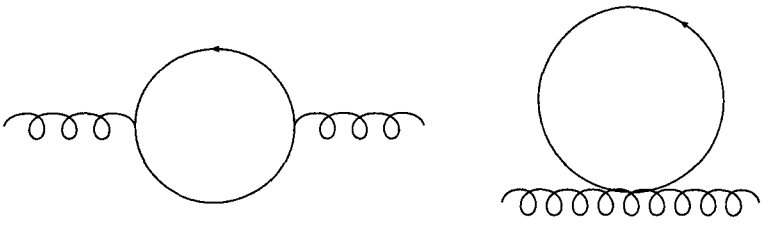

a *b*

Figure 5.3: Fermionic one-loop diagrams contribution to vacuum polarization. The tadpole diagram(b) is only present on lattice.

If we contract 5.11 with the polarization vectors of the A meson, only the first term will survives. Given the fact that we put the gluon on-shell $k^2 = 0$, we conclude that $\pi_{22} = 0$ in the continuum. It is thus expected that $g_0(am_q) = 0$ for any fixed am_q and hence has no logarithm or power divergence with regard to am_q.

The calculation has been done for ranges of am at $am_q = 0.1, 0.15, 0.2, 0.3 \ldots 1$ respectively. First of all, linearity with regards to $(am)^2$ has been demonstrated when am is small compared to am_q. One can refer to Fig. 5.4 to get a sense of the linearity. Also, unconstrained least square fits reveal that the $g_0(am_q)$ for different am_q are of order 10^{-8} while constrained fits[2] give 10^{-12}, which are essentially 0. Therefore we enforce $g_0(am_q) = 0$ in Eqn. 5.9. Constrained fits to the resulting form are performed to extract $g_2(am_q)$ for all am_q's and the results are summarized in Table 5.1.

The next step will be to fit the $g_2(am_q)$ obtained from previous fits to the form 5.9 in which we know $g_{2,-2} = 0$ now. By the same arguments in Section 4.3 one can conclude that the following relation needs to be hold in order to improve lattice gauge action with massless staggered quarks:

$$c_1^{(1)} - c_2^{(1)} = g_{2,0}^{(m_A)}. \tag{5.12}$$

The extrapolation to $m_q \to 0$ is necessary so that our results can make contact with MILC simulations with u,d and s quarks, where $am_q < 0.03$.

In the actual fitting, we found that several higher order terms with regard to am have to be included in order for us to get a decent χ^2 in the first step of fitting although their

[2]We expect $g_n(am_q)$ scales like $1/(n!(am_q)^{2n+2})$ and by applying the corresponding Bayesian prior we get a constrained fit.

Table 5.1: $g_2^{(m_A)}(am_q)$ for different am_q's are summarized. It is observed that the systematic errors are relatively larger for small am_q's.

am_q	$g_2^{(m_A)}(am_q)$
0.1	0.00364(1)
0.15	0.0036752(7)
0.2	0.003701(1)
0.3	0.003730711(1)
0.4	0.00372996(4)
0.5	0.003696507(2)
0.6	0.0036328671(4)
0.7	0.0035435429(3)
0.8	0.0034337690(4)
0.9	0.0033087971(2)
1.0	0.0031734700(3)

coefficients are generally not well-resolved. It is also observed that the fit results are very stable: a particular $g_2(am_q)$ changes by only $10^{-5} - 10^{-6}$ in an unconstrained fit if we leave one half of the data set out. They change on a similar scale if we vary the number of higher order terms included although χ^2 can look very bad. In the second step of the fit when we fit the set of $g_2(am_q)$'s to 5.9, the coefficients $g_{2,0}$ and $g_{2,2}$ change up to a few percents if we exclude the term $h_{2,2}\ln(am_q)(am_q)^2$ from the fit form or leave out several data points at *small* am_q(we have tried to leave out $am_q = 0.1, 0.15$ and 0.2). However, as one can see in Fig. 5.5, the signature of the presence of the logarithm term(the apparent dip) is clear. Since the systematic errors for each $g_2(am_q)$ are much smaller than a few percents, the change of $g_{2,0}^{(m_A)}$ after the exclusion of the smallest three am_q's from the data set is quoted as its systematic error. One can refer to Fig. 5.5 for the appearance of the data set and the fit. After performing all the fits, we get:

$$g_{2,0}^{(m_A)} = 0.00361(1). \tag{5.13}$$

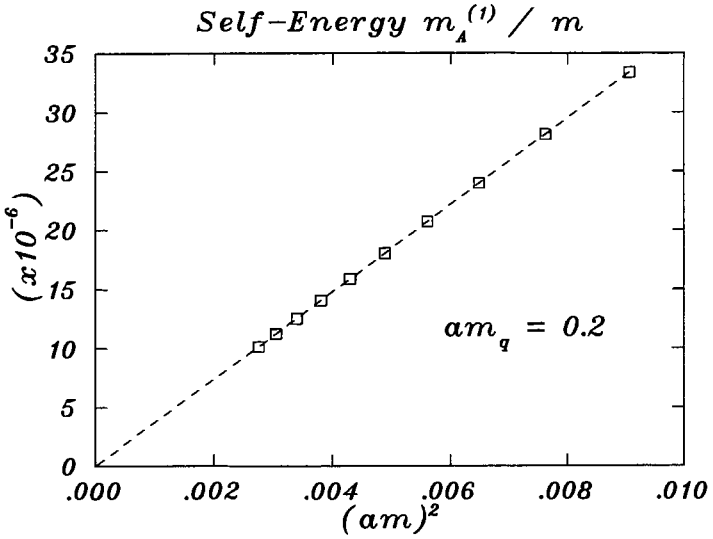

Figure 5.4: $m_A^{(1)}/m$ is displayed as a function of $(am)^2$ at $am_q = 0.2$. One can see the excellent linearity as predicted by Eqn. 5.7. The intercept of the curve with $m_A^{(1)}/m$ axis is shown to be 0 as well.

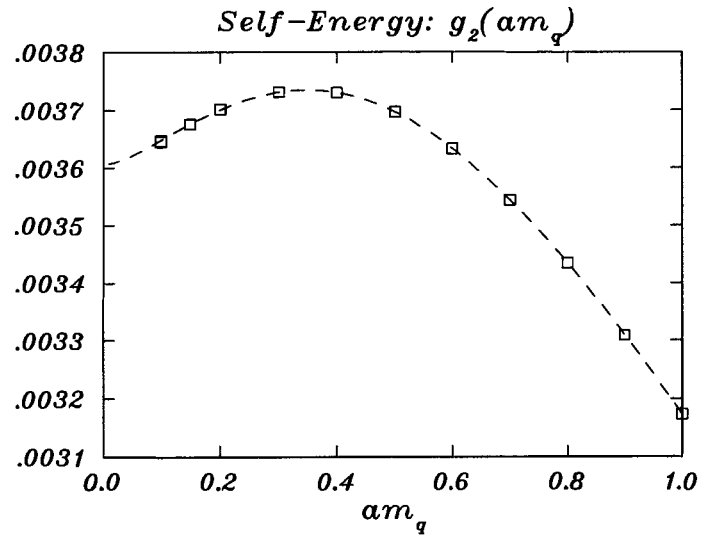

Figure 5.5: $g_2^{(m_A)}(am_q)$'s are displayed versus am_q. The dashed line is the fit result. It can be seen that a smooth limit exists as $am_q \to 0$.

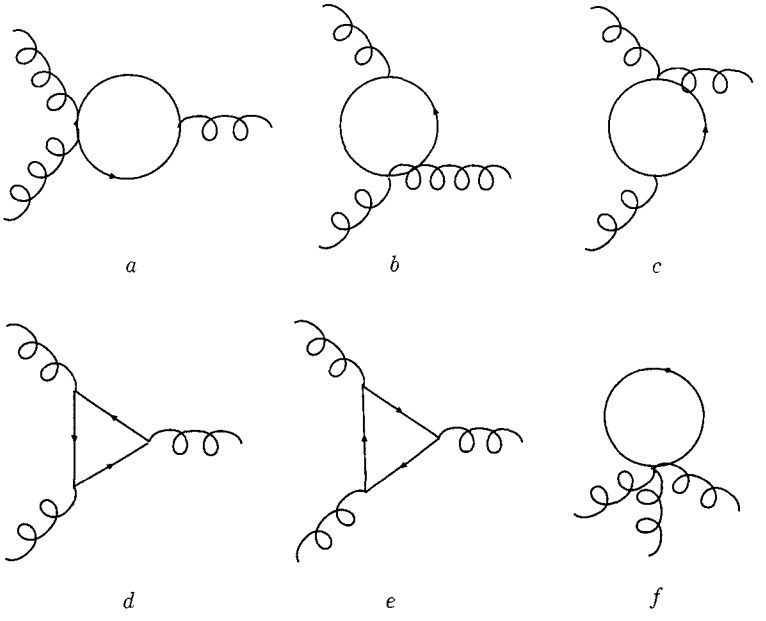

Figure 5.6: Fermion loop contributions to renormalization of 3-point coupling.

5.5 Renormalization of 3-point coupling

Similarly to the previous section, analytical results from corresponding sections in Chapter 4, namely Section 4.4, can be directly applied here. We again need some physical arguments regarding the continuum counterpart of 3-point coupling renormalization to determine the infrared behavior. First of all, the contribution of fermion loops in the QCD beta function is well-known:

$$\beta_f(am_q) = \frac{g^3 n_f}{24\pi^2} \ln(am_q), \tag{5.14}$$

where n_f is the number of flavors in our problem. We also know that in the tree level calculation we conclude $\lambda_{tree}/m \sim -8g$. Taking the fact that g is effectively 1 in our theory into account, $g_0(am_q)$ now contains a logarithm contribution looking like:

$$-\frac{n_f}{3\pi^2} \ln(am_q). \tag{5.15}$$

We have one flavor of quark now and can predict the logarithm term in $g_0(am_q)$ without difficulty.

Furthermore, we need to find out if there are any power divergences with regard to $(am_q)^2$. Again we perform a continuum calculation: in the continuum, only two triangular

diagrams(d,e in Fig. 5.6) contribute to the renormalization. Using the same momentum set-up as in Section 4.4, it is relatively straightforward to carry out the trace algebra by keeping only the m^3 term, which turns out to be just infrared divergent:

$$\frac{g^3 f^{abc} m^3}{240\pi^2 m_f^2}. \tag{5.16}$$

We should then normalize the contribution by the tree level factor which can be obtained by contracting the tree level vertex with the polarization vectors of the three gluons. After that, one obtains:

$$-\frac{g^2 m^2}{120\pi^2 m_f^2}. \tag{5.17}$$

It is then clear that there is a power divergent term $1/(am_q)^2$ in $g_2(am_q)$ and its coefficient is $-1/(120\pi^2)$. The power divergence should be the most severe divergence we expect in $O(a^0)$ terms. In summary, after the removal of the continuum like power divergence we expect the following relation to be satisfied in the limit of $am_q \to 0$:

$$4\left(9(c_1^{(1)} - c_2^{(1)}) + 2c_2^{(1)}\right) = -g_{2,0}^{(\lambda)}. \tag{5.18}$$

The actual calculation follows the same route as the previous section. We obtain $g_0(am_q)$ and $g_2(am_q)$ for a set of am_q's by fitting sets of data to 5.7 respectively. The results are summarized in Table 5.2. In the case of $g_0(am_q)$ the results show clear linearity with regard to $\ln(am_q)$ as in Fig. 5.7. Also, quantitatively an unconstrained least-squares fit gives the value of the coefficient of the logarithm term as -0.0329 while our formula predicts -0.0337. Given the fact that the range of am_q we are working on is not small enough to diminish higher order contributions, the value of coefficient we get is consistent with continuum theory's prediction. It serves as a very good internal check for our calculations. Moreover, Eqn. 5.8 dictates that after the removal of the logarithm term we should recover a second-order polynomial function of am_q. Indeed, it is again verified as shown in Fig. 5.8.

As for the $g_2(am_q)$ term, it is shown in Fig. 5.9 and 5.10 that $g_2(am_q)$ is not a simple quadratic function of am_q before we deal with the power divergence while after the removal of $1/(am_q)^2$ term $g_2(am_q)$ displays good quadratic behavior with regards to am_q, which is fully expected from 5.9.

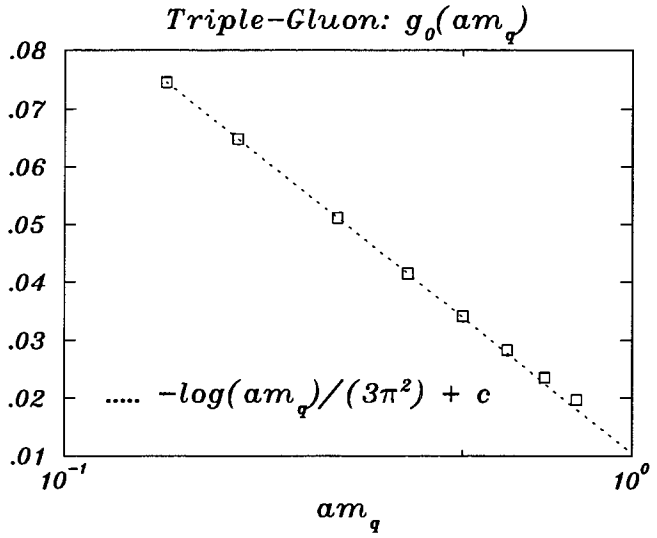

Figure 5.7: $g_0^{(\lambda)}(am_q)$'s are clearly linear with regarding to $\ln(am_q)$.The dashed line has the theoretical predicted slope while it is forced to go through the data point at the minimum am_q value. The agreement between the line and the data points is apparent.

We used the same approach to estimate the systematic errors $g_{0,0}^{(\lambda)}$ and $g_{2,0}^{(\lambda)}$ as for $g_{2,0}^{(m_A)}$ described in the previous section. The results are:

$$\begin{aligned} g_{0,0}^{(\lambda)} &= 0.01060(5), \\ g_{2,0}^{(\lambda)} &= -0.140(1). \end{aligned} \tag{5.19}$$

5.6 Accumulation and discussion of the results

Combining the Eqns 5.12, 5.18, 5.13 and 5.19, we can solve for $c_1^{(1)}$ and $c_2^{(1)}$:

$$\begin{aligned} c_1^{(1)} &= 0.00486(13), \\ c_2^{(1)} &= 0.00126(13). \end{aligned} \tag{5.20}$$

We need to transform our results into the form that is useful for the HPQCD collaboration as in Eqns. (6) and (7) in [53]. First let us use $c_i^{(1)}(i = 1,2,3)$ as the one-loop coefficients including both quenched and quark contributions. Now consider the general

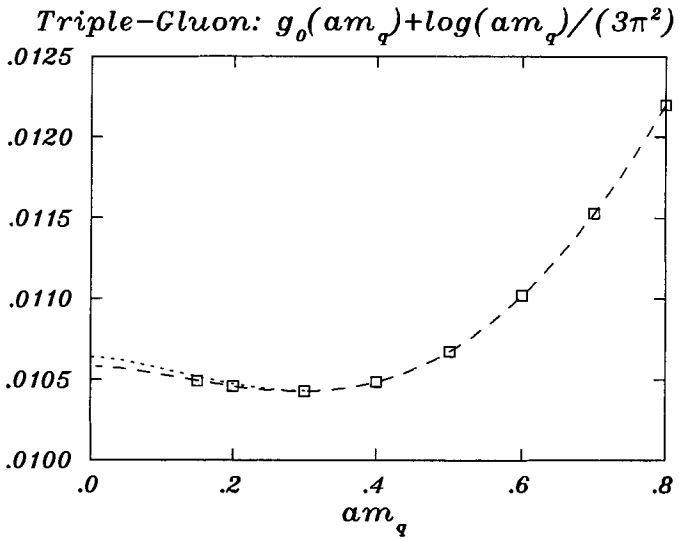

Figure 5.8: After removal of logarithm part from $g_0^{(\lambda)}(am_q)$, the data set shows quadratic behavior with regard to am_q. The dashed line is the fit to the full set of data while the dot line is the fit where three smallest am_q's are excluded.

form of the improved action as 4.4:

$$S[U] = \frac{2}{g^2}\sum_{i=0}^{3} c_i(g^2)S_i \equiv \sum_{i=0}^{3}\beta_i S_i.$$

From the discussion in Section 4.3 and 4.4 we know that:

$$\begin{aligned}
\beta_0 &= \frac{2}{g^2}\left(\frac{5}{3} + c_0^{(1)}g^2\right),\\
\beta_1 &= \frac{2}{g^2}\left(-\frac{1}{12} + c_1^{(1)}g^2\right),\\
\beta_2 &= \frac{2}{g^2}c_2^{(1)}g^2,\\
\beta_3 &= 0.
\end{aligned} \tag{5.21}$$

By some simple algebra we have:

$$\begin{aligned}
\beta_1 &= -\frac{\beta_0}{20}\left(1 - 4\pi(\frac{3}{5}c_0^{(1)} + 12c_1^{(1)})\alpha_s\right),\\
\beta_2 &= \frac{12\pi\beta_0}{5}c_2^{(1)}\alpha_s.
\end{aligned} \tag{5.22}$$

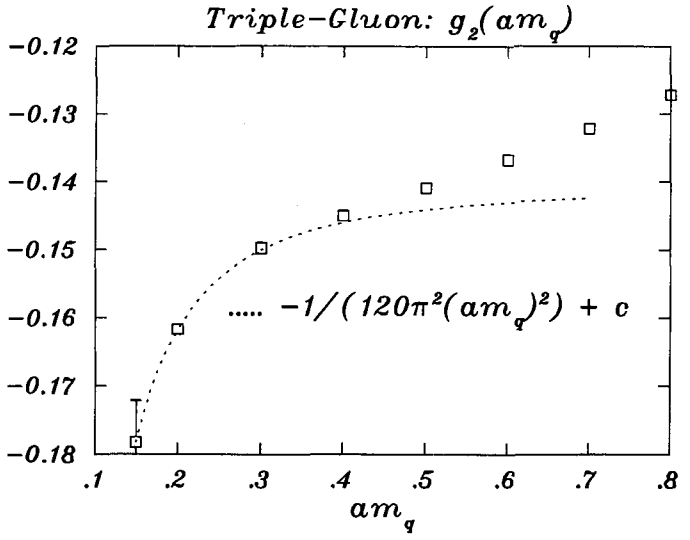

Figure 5.9: $g_2^{(\lambda)}(am_q)$ is displayed as the function of am_q before the removal of power divergence. The dashed line is predicted by theory while constant c is fixed by forcing the line go through the data point at minimum am_q. It is seen that at small am_q's the infrared power divergence is the dominant term.

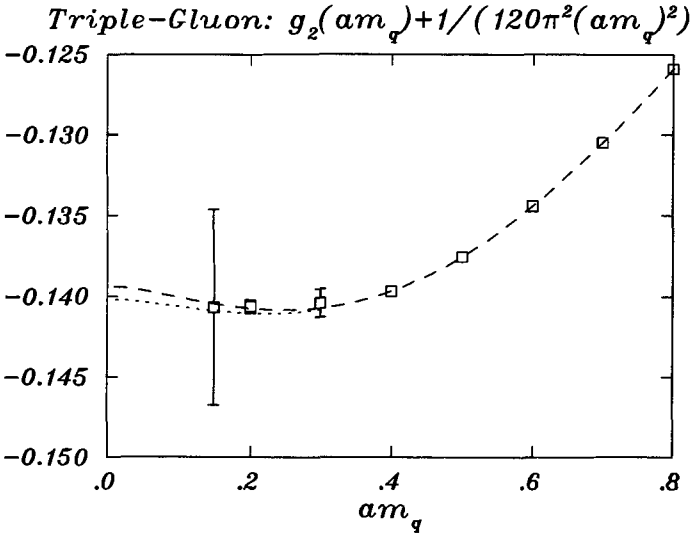

Figure 5.10: After the proper elimination of $1/(am_q)^2$ term in $g_2^{(\lambda)}(am_q)$, it appears now a quadratic function of am_q. The dashed line and the dot line have the same meaning as in Fig. 5.8

Table 5.2: $g_0^{(\lambda)}(am_q)$'s and $g_2^{(\lambda)}(am_q)$'s are summarized for different am_q's. It is noticed that systematic errors are generally larger for small am_q's.

am_q	$g_0^{(\lambda)}(am_q)$	$g_2^{(\lambda)}(am_q)$
0.15	0.07456(1)	−0.178(6)
0.2	0.0648161(5)	−0.1617(4)
0.3	0.051090(2)	−0.1498(9)
0.4	0.0414332(1)	−0.14498(6)
0.5	0.03408572(2)	−0.140933(7)
0.6	0.028272563(9)	−0.136776(2)
0.7	0.023575013(4)	−0.132222(1)
0.8	0.019733513(1)	−0.12722(3)

Taking the Tadpole improvement[27] into account, the mean link can be expanded as follows:

$$u_0 = 1 + u_0^{(1)}\alpha_s + O(\alpha_s^2). \tag{5.23}$$

We can now rewrite 5.22 into the following:

$$\begin{aligned} \beta_1 &= -\frac{\beta_0}{20u_0^2}\left(1 - 4\pi(\frac{3}{5}c_0^{(1)} + 12c_1^{(1)})\alpha_s + 2u_0^{(1)}\alpha_s\right), \\ \beta_2 &= \frac{12\pi\beta_0}{5u_0^2}c_2^{(1)}\alpha_s. \end{aligned} \tag{5.24}$$

Also, according to the normalization relation 4.5 and the fact that c_3 can be set to 0 in all orders of perturbation theory, we have the following relation between the one-loop improvement coefficients:

$$c_0^{(1)} + 8c_1^{(1)} + 8c_2^{(1)} = 0. \tag{5.25}$$

We are ready now to derive the final formula. Given the fact that all the quenched contribution and Tadpole contribution were calculated in [53], we can simplify 5.24 into the

following:

$$\begin{aligned}\beta_1 &= -\frac{\beta_0}{20u_0^2}\left(1+0.4805\alpha_s - 4\pi(\frac{3}{5}c_0^{(1)}+12c_1^{(1)})\alpha_s\right),\\ \beta_2 &= -\frac{\beta_0}{u_0^2}\left(0.033\alpha_s - \frac{12\pi}{5}c_2^{(1)}\alpha_s\right)\end{aligned} \tag{5.26}$$

where now all the one-loop coefficients contain *only* quark loop contributions. After plugging the numbers in 5.20

$$\begin{aligned}\beta_1 &= -\frac{\beta_0}{20u_0^2}\left(1+0.4805\alpha_s - 0.3637(14)N_f\alpha_s\right),\\ \beta_2 &= -\frac{\beta_0}{u_0^2}(0.033\alpha_s - 0.009(1)N_f\alpha_s),\end{aligned} \tag{5.27}$$

where N_f is the number of flavors. Since we calculated the contributions to the improvement coefficients from one flavor, the contributions from N_f flavors can be obtained in 5.20 under the assumption that a flavor symmetry is present in the sea quark sector. The assumption is widely adopted in experiments and phenomenological calculations.

It is observed that the corrections of improvement coefficients from sea quark contributions are significant for $N_f = 3$. These missing pieces can be responsible for the large scaling violations observed.

Chapter 6

Summary and conclusion

Motivated by the somewhat larger scaling violations in unquenched static quark potentials than the quenched case, we performed the un-quenched improvement of the Lattice Gauge Action. We generally followed the approach of Lüscher and Weisz[12] by requiring only on-shell quantities to be improved. It was pointed out by Lüscher and Weisz that we need only two operators with independent coefficients present in the counter-term if only order a^2 improvement is pursued. A particular space-time geometrical setting, namely the twist world, provided us with two on-shell quantities that are relatively simple to calculate. Perturbative calculations were performed for both of the on-shell quantities and the one-loop improvement coefficients were fixed accordingly.

There was one major complication in our calculations compared to the quenched calculations done by Lüscher and Weisz: we have one more energy scale m_q present in our question. The complication manifests itself in many different ways: first of all, careful considerations must be taken to understand the physical meanings of different orders of limits for which different calculation processes need to be designed; second of all, it's relatively hard for us to estimate the systematic errors since some higher order terms in our expansions are suppressed only by $(m/m_q)^2$ and the convergence of the expansion is relatively poor; thirdly the calculations become more and more expensive as m_q decreases since m must be kept to be (much) smaller than m_q in order for us to get a good fit. Despite the larger computational burden of the calculation for fermionic loops (the entire project required about 300 – 500 CPU days on the Fermilab lattice QCD cluster), sufficiently accurate results were obtained for the improvement coefficients at small quark masses, of relevance to state-of-the

art simulations by the MILC collaboration.

Finally, it was observed that the quark loop contributions to the improvement coefficients are significant if there are three flavors of sea quark present. These contributions can be responsible for the large scaling violations observed in the static quark potential. Furthermore, now we have a complete one-loop improved lattice gauge action at our disposal. The action should prove to be useful in future high precision un-quenched lattice simulations.

Bibliography

[1] David J. Griffths, *Introduction to elementary particle physics*, Wiley, NY, 1987. An uptodate review is given by David Charlton, *Experimental Tests of the Standard Model* arXiv:hep-ex/0110086.

[2] A good review on physics beyond standard model is given by R. D. Peccei, *Physics Beyond Standard Model* arXiv:hep-ph/9909233.

[3] A good review on LHC physics is given by N.V. Krasnikov and V. A. Matveev, *Search for new physics at LHC* arXiv:hep-ph/0309200.

[4] R. D. Peccei, *Discrete and Global Symmetries in Particle Physics* arXiv:hep-ph/9807516.

[5] Interested readers can refer to C. D. Froggatt, *The Origin of Mass* arXiv:hep-ph/0307138.

[6] Adriano Di Giacomo, *Confinement in QCD: Results and Open problems* arXiv:hep-lat/0510065.

[7] A brief review is given by Barry R. Holstein, *A Brief Introduction to Chiral Perturbation Theory* arXiv:hep-ph/9911449. A more detailed accout can be found in *Aspects of Chiral Symmetry* by A. V. Smlga, arXiv:hep-ph/0010049. Importance and application of chiral symmetry on lattice is reviewed by S. Chandrasekharan and U.-J. Wiese in *An Introduction to Chiral Symmetry on Lattice* arXiv:hep-lat/0405024.

[8] For a simple introduction to QCD, one can refer to *Introduction to QCD* by P. Nason, lecture notes for the 1997 European School of High-Energy Physics, 25 May - 7 Jun

1997, Menstrup, Denmark, report CERN-98-03. An updated version could be find on the website of P. Nason.

[9] A review is given by Zoltan Ligeti, *The CKM matrix and CP violation(in the contiuum approximation)* arXiv:hep-lat/0601022.

[10] The subject of glueball is reviewed by Geoffrey B. West, *The Glueball: The Fundamental Particle of Non-perturbative QCD* arXiv:hep-ph/9608258.

[11] Kenneth G. Wilson, *Confinement of Quarks*, Phys. Rev. D 10 (1974), 2445.

[12] M. Lüscher and P. Weisz, Nucl. Phys. B266 (1986), 309.

[13] C. T. H. Davies, private communication.

[14] M. Lüscher and P. Weisz, *On-shell Improvement Lattice Gauge Theoryies*, Commun. Math. Phys. 97 (1985), 59-77.

[15] A brief account of history of LQCD can be found in P. Hasenfratz, *Chiral symmetry on the lattice* arXiv:hep-lat/0406033.

[16] Michael E. Peskin and Daniel V. Shroedoer, *Introduction to Quantum Field Theory*, Westview, TN, 1995.

[17] A review of Euclidean Field Theory is given by Francesco Guerra, *Euclidean Field Theory* arXiv:hep-ph/0510087.

[18] G. C. Wick, Phys. Rev. 96 (1954),1124; J. Schwinger, Phys. Rev. 115 (1959)721.

[19] A good account of role of lattice regularizaton can be found in *The theoretical background and properties of perfect action* by P. Hasenfratz, arXiv:hep-lat/9803027.

[20] Steven Weinberg, *The Quantum Theory of Fields*, Volume 1, Cambridge University Press, Cambridge, UK , 1995.

[21] Matthew A. Nobes, *Automated Lattice Perturbation Theory for Improved Quark and Gluon Actions*, PhD Thesis, Simon Fraser University, 2004.

[22] M. Lüscher and P. Weisz, Phys. Lett. B, 158B (1985), 250.

[23] M. García Pérez, J. Snippe and P. van Baal, Phys. Lett. B, 389 (1996), 112. J. Snippe, Phys. Lett. B, 389 (1996), 119.

[24] H. B. Nielser, M. Ninomiya, Phys. Lett. B 105 (1981), 219.

[25] M. Lüscher, Phys. Lett. B 428 (1998), 342.

[26] J. B. Kogut and L. Susskind, Phys. Rev. D 11 (1975), 395.

[27] G. Peter Lepage and Paul B. Mackenzie, Phys. Rev. D, 48 (1993), 2250.

[28] For a recent review refer to *Theoretical issues with staggered fermion simulations* by Stephan Dürr, arXiv:hep-lat/0509026.

[29] For a recent discussion about fourth root trick, one can refer to *Staggered Chiral Perturbation Theory and the Fourth-Root Trick* by C. Bernard, arXiv:hep-lat/0603011.

[30] Stephen R. Sharpe, *Rooted Staggered Fermions: Good, Bad or Ugly?*, talk given in Lattice 2006.

[31] M. Lüscher, JHEP 0305 (2003), 052(arXiv:hep-lat/0304007).

[32] S. Duane, A. D. Kennedy, B. J. Pendleton and D. Roweth, *Hybrid Monte Carlo*, Phys. Lettt. B 195 (1987),216.

[33] M. Lüscher, Comput. Phys. Commun. 165 (2005), 199(arXiv:hep-lat/0409106).

[34] Roberto Frezzotti, Pietro Antonio Grassi, Stefan Sint and Peter Weisz, Nucl. Phys. B(Proc. Suppl.) 83-84 (2000), 941-946.

[35] P. Hasenfratz and F. Niedermayer, Nucl. Phys. B 414 (1994), 785.

[36] David B. Kaplan, Phys. Lett B 288 (1992), 342. For a review, one couild refer to *Domain Wall Fermions and Chiral Gauge Theories* by Karl Jansen, arXiv:hep-lat/9410018.

[37] R. Narayanan and H. Neuberger, Phys, Lett. B 302 (1993), 62. A review can be found in *Regulated Chiral Gauge Theory* by H. Neuberger, arXiv:hep-lat/0011035.

[38] A good review of Lattice Perturbation Theory can be found in *Lattice Perturbation Theory* by Stefano Capitani, arXiv:hep-lat/0211036.

[39] There are a lot of textbooks of LQCD. For example, M. Creutz, *Quarks, Gluons, and Lattices*, Cambridge University Press, Cambridge, UK, 1983. A good introductory review article is written by Rajan Gupta: *Introduction to Latiice QCD*, arXiv:hep-lat/9807028.

[40] M. Lüscher, *Selected Topics In Lattice Field Theory*, Lectures at the 1988 Les Houches Summer School, North Holland, 1990.

[41] John B. Kogut, Rev. Mod. Phys, 55 (1983), 775.

[42] D. G. Boulware, *Renormalizability of Massive Non-Abelian Gauge Theories: A Functional Integral Approach*, Annals Phys. 56 (1970),140. For a more pedagogical review, one can refer to Heinz J. Rothe, *Lattice Gauge Theories An Introduction*, third edition(2005), World Scientific Lecture Notes in Physics- Vol.74.

[43] Howard D. Trotter, *Higher-order Perturbation Theory for highly-improved actions: Techniques and results*, Talk given at Lattice 2003.

[44] A. Hart et al., J.Comput.Phys. 209 (2005), 340.

[45] Colin J. Morningstar, Phys. Rev. D, 48 (1993), 2265.

[46] G. 't Hooft, Nucl. Phys. B 153 (1979), 141.

[47] Norman Harold Shakespeare, *Simulation of Non-Relativistic Quantum Chromodynamics at strong and weak coupling*, PhD thesis, Simon Fraser Universtiy, 2000.

[48] P. van Baal, Comm. Math. Phys, 92 (1983),1.

[49] K. Symanzik, Nucl. Phys. B 226 (1983), 187.

[50] J. Snippe, Nucl. Phys. B, 498 (1997), 347-396.

[51] R. Wohlert, *Improved Continuum Limit Lattice Action for Quarks*, Desy 87-069.

[52] G. Peter Lepage, Phys. Rev. D, 59 (1999), 074502.

[53] M. Alford et al, Phys. Lett. B, 361 (1995), 87.